PROGRESS REPORT

For Period January 1 through March 31, 1962
AEC R&D Contract AT(30-1)-2389

DEVELOPMENT OF PLUTONIUM-BEARING FUEL MATERIALS

NUMEC P-100

Nuclear Materials and Equipment Corporation
Apollo, Pennsylvania

~~For Official Use Only, Pending Patent Release~~

DISCLAIMER

External Distribution List

U. S. Atomic Energy Commission, New York Operations Office
- M. Balicki
- H. S. Potter
- Vincent Siuta
- Leonard Topper
- Seymour Zirin

U. S. Atomic Energy Commission, Washington
- F. Charles Moesel (2)
- J. M. Simmons (5)
- M. Whitman
- M. Zeibold
- Reports and Statistics Branch

U. S. Atomic Energy Commission, Chicago Operations Office
- Bruce Anderson

U. S. Atomic Energy Commission, National Laboratories
- F. Foote, Argonne
- H. Young, Argonne (4)
- E. Childs, Dow Chemical
- E. A. Eschbach, Hanford
- E. A. Evans, Hanford
- W. K. Woods, Hanford
- O. J. Wick, Hanford
- J. Musser, Hanford
- I. D. Thomas, Hanford
- W. Cashin, KAPL
- H. Rizzo, Lawrence Radiation (3)
- R. D. Baker, Los Alamos
- L. B. Jones, Mound
- R. L. Mettler, Oak Ridge (3)
- D. F. Cope, Oak Ridge
- E. S. Bomar, Oak Ridge
- E. J. Kreh, Westinghouse-Bettis

U. S. Atomic Energy Commission, Contractors
- W. J. O'Leary, Allis Chalmers Manufacturing Company
- R. W. Dayton, Battelle
- W. Duckworth, Battelle
- G. M. Butler, Jr., Carborundum Company
- R. H. Gale, Combustion Engineering
- A. D. Schwope, Clevite Research Center
- L. A. Matheson, Dow Chemical Company
- W. Alter, General Electric Company, Vallecitos
- L. D. Harris, National Carbon Company
- A. Strasser, Nuclear Development Corporation of America
- R. W. Hartwell, Power Reactor Development Company
- D. E. Hamby, Union Carbide Metals Company
- C. W. Kuhlman, United Nuclear Corporation
- Olin Mathieson Chemical Corporation

NUMEC Distribution List

R. J. Atkins
A. Biancheria
F. M. Cain
C. S. Caldwell
J. Eck
G. Ehrlich
F. Forscher
R. Frumermann
H. J. Garber
E. E. Garcia
J. Goodman
O. S. Gray
E. K. Halteman
R. M. Horgos
M. D. Houston
L. A. Hughes
R. A. Jaroszeski
L. J. Jones
W. Judd
A. Kasberg
H. Krake
A. L. Maharam
J. Marley
O. Menis
J. Miles
L. P. Pepkowitz
K. H. Puechl
P. Rey
W. G. Ross
J. Ruzbacki
J. Scott
Z. M. Shapiro
F. Shipko
J. Stoner
M. M. Turkanis
B. Vondra
L. Weber
A. M. Weis
M. Zambernard
Library (5)

Previous Quarterly Progress Reports issued in this series are:

Number	For the Period Ending
NUMEC P-10	December 31, 1959
NUMEC P-20	March 31, 1960
NUMEC P-30	June 30, 1960
NUMEC P-40	September 30, 1960
NUMEC P-50	December 31, 1960
NUMEC P-60	March 31, 1961
NUMEC P-70	June 30, 1961
NUMEC P-80	September 30, 1961
NUMEC P-90	December 31, 1961

TABLE OF CONTENTS

PROJECT AND FACILITY ADMINISTRATION

Task 1.00

K. H. Puechl

Summary of Development Activities

During this reporting period, particular effort has been placed on powder blending and pellet sintering studies prior to irradiation sample fabrication, and, subsequently, the production and characterization of the pellets slated for irradiation. Also, PuO_2 and UO_2-PuO_2 characterization studies have been continued, and new techniques are being developed. Specifically, dynamic moisture pickup determinations on PuO_2 have been made in moist air, nitrogen, and carbon dioxide atmospheres using a recording thermogravimetric balance; the Sharples Micromerograph has been committed to plutonium, and powder particle size distributions have been measured and compared to previous determinations made with air-permeability equipment; and the suitability and reliability of analytical chemistry assaying procedures such as x-ray fluorescence and gamma spectrometry are being evaluated. Prototype work on UO_2 for the direct precipitation of PuO_2 and PuO_2-UO_2 feed materials for swaging, vibratory compaction, and dispersion fabrication has also been continued. In addition, investigation of PuO_2 spherical particle formation by mechanical buildup and by plasma torch fusion has been extended. Associated reactor physics studies have been concentrated on the further comparison of plutonium and U-235 in near-thermal converter reactors.

In preparation for the fabrication of irradiation test specimens to be prepared by the mechanical blending of individual PuO_2 and UO_2 powders, blending studies were initiated to develop methods required for the attainment of desired homogeneity. Initial blending trials in a twin-shell blender were unsatisfactory due to balling up of the individual powders. These balls tended to remain intact through the pellet sintering fabrication step. It was further determined that these balls could not be broken up by hammermilling following blending. Good results were finally achieved by wet ball milling; the resultant pellets cannot be differentiated from pellets produced with coprecipitated material.

Pellet sintering studies on UO_2-5 w/o PuO_2 and UO_2-0.5 w/o PuO_2 were carried out to investigate the effect of compaction pressure, firing temperature, and firing time. Over the ranges of the parameters investigated, only minor trends were noted. In general, the resulting pellets were all satisfactory, having densities in the range 92.3 to 95.5% of theoretical. Also, it was determined that the glassy surface previously noted[1] was due to buildup

---

(i) NUMEC P-90, Progress Report, "Development of Plutonium-Bearing Fuel Materials", page 2.

within the furnaces of impurities contained in the as-received plutonium nitrate solution. The furnaces have been cleaned up, and the impurity problem is being resolved with the plutonium supplier.

Sintering studies have also been carried out on PuO_2 to study the effects of compaction pressure, firing temperature, firing time, and firing atmosphere. It has been determined that 1400-1500°C is the best firing temperature to obtain maximum pellet density, and also that sintering in air yields higher densities than sintering in a N_2-H_2 atmosphere. Further, it was noted that the degree of Pu_2O_3 formation while sintering in an N_2-H_2 atmosphere is inversely proportional to compaction pressure, indicating that the degree of formation is determined by the exposed surface area.

All pellets for the rabbit irradiation tests have been produced during this period. This includes using coprecipitated as well as mechanically blended feed material. For all pellets, the final densities were at least as high as specified.

In order to allow further assessment of the moisture pickup problem during PuO_2 powder handling and storage, the static atmosphere tests reported previously(i) were augmented by dynamic tests using a thermogravimetric balance. Measurements made in air, nitrogen, and carbon dioxide at 76% relative humidity and a 0.5 SCFH flow rate indicate that there are no major effects due to oxygen or carbon dioxide.

The Sharples Micromerograph has been committed to plutonium during this quarter, and preliminary investigations have been carried out to determine particle size distributions of plutonium oxide and precursor plutonium oxalate powders. Good reproducibility was attainable, and agreement with previous air permeability average particle size results was obtained. This gives indication that the Micromerograph can be used as a rapid method for quality control.

Two additional lots of UO_2-5 w/o PuO_2 powder were precipitated during this period. Powder characterization data for these and two previously produced lots have been obtained. Also, powder characteristics were remeasured following hammermilling in order to allow assessment of the effects of this treatment.

Assaying solids for plutonium content has been carried out by x-ray fluorescence examination. In addition, gamma ray spectrometry has also been extended to solids. Calibration curves have been generated for both methods. X-ray fluorescence appears particularly promising; reproducibility is good, and interference from common inert elements is small.

(i) NUMEC P-90, Progress Report, "Development of Plutonium-Bearing Fuel Materials", page 13.

In preparation for work with PuO_2 and UO_2-PuO_2, prototype studies are being carried out with UO_2 to assess the possibility of producing directly high density granular feed for swaging, vibratory compaction, and dispersion fuel fabrication. Trial precipitations have been carried out by the peroxide route, the homogeneous (urea) route, and the uranyl oxalate route. The products have been analyzed by optical and electron microscopy and densities, and particle sizes have also been measured.

Effort has been continued on the fabrication of spherical PuO_2 particles by mechanical buildup and also by plasma torch fusion. Mechanical buildup studies have been carried out using a variety of preconditioned powders in order to obtain an understanding of the parameters that influence reproducibility. The results are being evaluated. The plasma torch feeding mechanism has been modified, and subsequent trial runs under different torch and flow gas conditions indicate that a broad variety of product can be obtained. Of special interest is the fact that particles have now been produced that do not contain central voids; these particles are nearly 100% dense.

Reactor physics studies have been continued to allow assessment of plutonium relative to U-235 in near-thermal reactor systems. Under cost assumptions used previously[1], it has been shown that optimum fuel cycle costs from plutonium-natural uranium fueled systems are well below those attainable with slightly enriched uranium fueled systems even if it is assumed that radiation damage is not limiting and that an ideal burnable poison (or solution poison) exists to limit the reactivity.

General Plant Operations

The NUMEC Plutonium Laboratory has now been in operation with plutonium for more than one year. During this time interval, more than 16 kilograms of plutonium have been processed. Operating experience has been excellent. No one has received an exposure greater than allowable under Federal regulations. Minor contamination has occurred on a number of instances, but decontamination was readily achieved. This experience demonstrates that plutonium can be safely handled in an industrial-type operation, wherein the majority of employees are scientifically untrained.

Equipment design and installation is continuing in order to allow fabrication of fuel elements by swaging and rolling and also to allow post-irradiation examination of plutonium-containing materials within the hot cell facilities. The alpha boxes for the hot cell are on hand and are being outfitted to serve a variety of functions, including element disassembly, examination, sectioning, polishing, fission gas release determination, etc.

---

(1) K. Puechl, "Potential of Plutonium as a Fuel in Near-Thermal Converter Reactors", Nuclear Sci. and Eng., 12, 135-150 (1962).

Plans to utilize the Westinghouse Testing Reactor for all irradiations are now being changed due to the shutdown of this installation. Other reactor sites are being considered on the basis of technical requirements and possible shipping and travel expenditures.

PREPARATION AND CHARACTERIZATION OF FUEL MATERIALS

Task 2.00

C. S. Caldwell O. Menis

Plutonium Oxide Preparation via Oxalate Process and Resultant Powder Characterization

(C. S. Caldwell, A. Biancheria)

During this reporting period, no additional PuO_2 was processed; however, characterization studies were continued using material previously prepared. Short-term dynamic measurements of moisture adsorption on PuO_2 were made in a thermogravimetric balance using air, nitrogen, and carbon dioxide as the carrier gas. In addition, particle size determinations of PuO_2 and the precursor plutonium oxalate powders were made with the Sharples Micromerograph, and the results were compared to previous values determined with an air-permeability apparatus.

Moisture Adsorption in Plutonium Dioxide Powder

To supplement the long-term environmental moisture pickup studies reported previously for PuO_2 powder(i), short-term dynamic measurements, using different carrier gases, have been made using a recording thermobalance. The results of these studies will be the determination of limits of moisture pickup to be expected with PuO_2 powders of different surface areas under different conditions of atmospheric humidity.

Investigations during this period were carried out at room temperature using Samples 297-Pu-4-1 and 297-Pu-4-5 having surface areas of 60 and 10 M^2/gm, resp. Dynamic atmospheres of air, nitrogen, and carbon dioxide were used at 76% relative humidity and a flow rate of 0.5 SCFH. This relative humidity was achieved by bubbling the gases through two columns of saturated potassium sulfate solution.

To obtain base weights, the PuO_2 powders were dried to constant weight in the thermobalance at 115 to 120°C in a stream of dry nitrogen prior to and at the end of each experiment. Corrections for buoyancy differences were also applied to the raw data. The results are shown in Figure 2.1.

Although the final rate of approach to equilibrium was slightly slower in the moist CO_2 atmosphere than in moist air or nitrogen for Sample 297-Pu-4-1, the curves are nearly equivalent, indicating that there are no major effects due to O_2 or CO_2. The equilibrium moisture contents obtained from these

---

(i) NUMEC P-90, Progress Report, "Development of Plutonium-Bearing Fuel Materials", page 13.

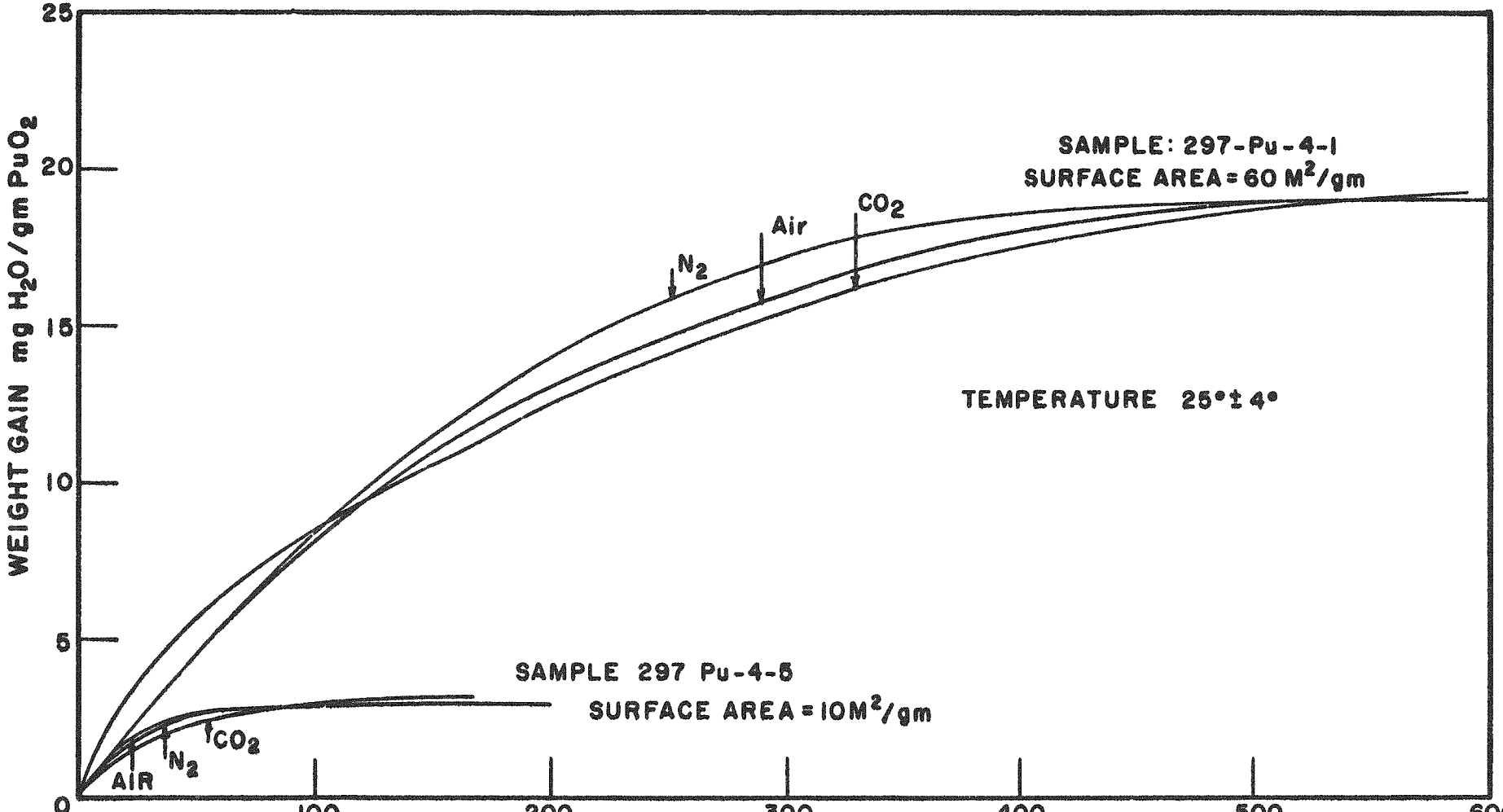

Figure 2.1

WATER ADSORPTION RATES FOR PuO_2 POWDER
EXPOSED TO VARIOUS ATMOSPHERES AT 76% RELATIVE HUMIDITY

curves are 19.0 mg H_2O/gm PuO_2 for the Pu-4-1 sample and 3.0 mg H_2O/gm PuO_2 for the Pu-4-5 sample. For practical purposes, the rate of adsorption during the first ten minutes of exposure in air can be considered equivalent for both samples, indicating that the moisture content for high surface area powders can be kept to a reasonable level if the cumulative exposure time is limited. Similar measurements employing samples with lower surface areas will be made at lower humidities to provide information applicable to a wider range of PuO_2 powders and atmospheric conditions of interest.

Particle Size Determination of Plutonium Dioxide and Plutonium Oxalate Powders

Installation of the Sharples Micromerograph air-sedimentation equipment into a glove box was completed during this period, and trial measurements were made on PuO_2 and $Pu(C_2O_4)_2$ powders.

Particle size distributions of several PuO_2 samples were measured over a wide range of nitrogen feed pressures to determine optimum dispersion conditions. Feed pressures of 100-125 psig were found to yield satisfactory dispersions for all powders tested, although some dependence on powder history was observed. Agreement of the PuO_2 Micromerograph average particle sizes with previously measured air-permeability average sizes[i] is encouraging and supports the conclusion that adequate dispersion was obtained. Good reproducibility was also attainable (see Figure 2.2) indicating that this method can successfully be used for routine particle-size control.

Preliminary trials using precursor plutonium oxalates (aged in an air atmosphere) were also carried out. These particle size data are compared in Table 2.1 with values obtained for the corresponding PuO_2 powders. This comparison shows that significant particle degradation occurs during calcination of the oxalate, an effect observed previously using air-permeability measurement[ii].

Preparation and Characterization of Mixed Plutonium-Uranium Oxides
(A. Biancheria, G. Ehrlich, E. Garcia, J. Goodman, R. Jaroszeski)

During this period, four lots of UO_2-5 w/o PuO_2 were prepared by coprecipitation to provide additional material for pellet fabrication studies and for irradiation sample preparation. These products were characterized to establish process controllability and to ascertain supplementary

---

(i) NUMEC P-90, Progress Report, "Development of Plutonium-Bearing Fuel Materials", page 7.

(ii) NUMEC P-90, Progress Report, "Development of Plutonium-Bearing Fuel Materials", page 31.

Table 2.1

Comparison of Precursor Plutonium Oxalate
Particle Size with Corresponding Plutonium Dioxide Size

Sample Identification	Micromerograph Average* Particle Size, microns	
	$Pu(C_2O_4)_2$	PuO_2
297-Pu-9-Lot II	6.5	1.7
297-Pu-9-Lot III	5.8	2.9
297-Pu-9-Lot IV	3.8	2.6
297-Pu-11A	6.1	2.9
297-Pu-11B	4.8	2.4

* Feed pressure of 125 psig

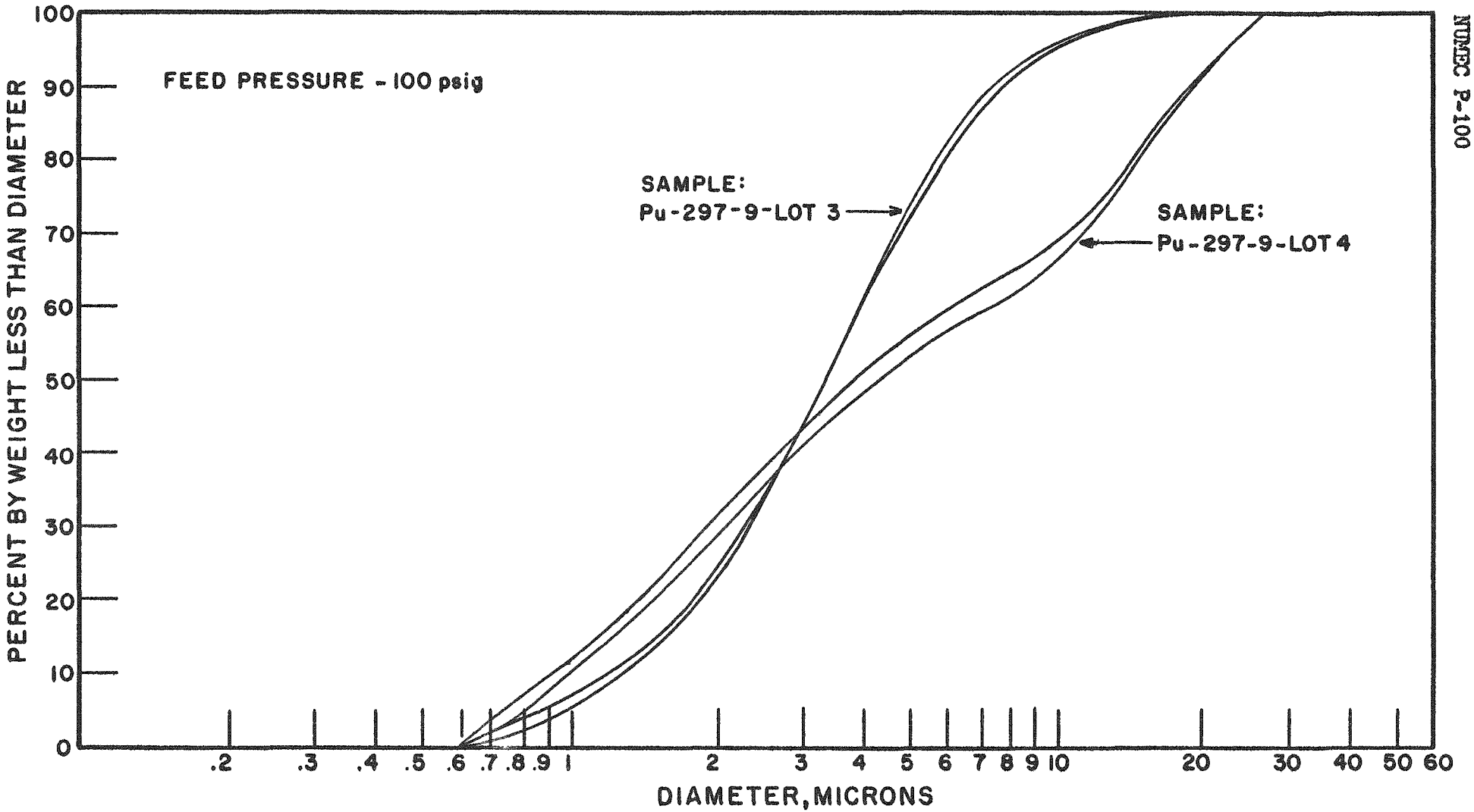

Figure 2.2

REPLICATE AIR-SEDIMENTATION
PARTICLE SIZE ANALYSES OF PuO_2 POWDERS

(MICROMEROGRAPH METHOD)

information, including the effect of hammermilling on particle size. In addition, trial blends of UO_2-20 w/o PuO_2 and UO_2-5 w/o PuO_2 were prepared by physical mixing of UO_2 and PuO_2 powders using dry and wet processes. From this work, it was established that homogeneity requirements for irradiation sample fabrication could be met by wet ball milling.

Continuous Coprecipitation and Product Characterization of UO_2-5 w/o PuO_2

Lots 871-A-3A and 871-A-3B were prepared by a previously used method; i.e., continuous precipitation from an acidified U(VI)-Pu(IV) nitrate solution with concentrated aqueous ammonia. Processing data for these 350 gm preparations as well as for two other batches described below are presented in Table 2.2. The resultant powder contained a substantial percentage of +200 mesh hard agglomerates which could not be broken down by the standard shaker dispersion technique used prior to sedimentation particle size analysis; however, hammermilling once through 0.010" herringbone screens was found to be partially effective. The effect of hammermilling on powder characteristics is shown in Table 2.3. These data agree well with those obtained previously on similarly treated material (Lots 871-A-1 and 871-A-2)(i). The results indicate that hammermilling may be required as a normal processing step, possibly in combination with alternate precipitation and/or washing procedures, in order to eliminate the presence of undesirable hard agglomerates in the pelletizing feed.

Two other lots of UO_2-5 w/o PuO_2 powder (297-Pu-14A and 297-Pu-14B) were prepared by continuous coprecipitation under the conditions also shown in Table 2.2. In addition to the original 740°C reduction step, a second full reduction cycle at 640°C was required to obtain complete conversion. Since the product surface area was 50% higher than anticipated, subsequent heat treatments were used in an attempt to reduce the surface area to 5 ± 1 M^2/mg. Such heat treatment was carried out at temperatures of 740, 780, 820, 860, and 900°C in a reducing atmosphere. Contrary to results obtained with previous preparations, the surface area of this material did not decrease substantially, as can be seen from the data presented in Table 2.4. However, the air-permeability particle size showed an increase which may be attributed to particle-particle bridging. In addition, one cycle of oxidation-reduction treatment at 780°C (Sample 14A-780(RR)) was carried out. This resulted in a 37% decrease in surface area which may be attributed to reaction heating effects during the oxidation step. Due to the abnormal characteristics observed in the above material, further evaluation will be carried out, including sinterability tests and electron microscopy.

Blending of PuO_2 and UO_2 Powders

In preparation for providing mechanically blended PuO_2-UO_2 for rabbit tests, mixing trials were carried out using various blending and milling techniques.

(i) NUMEC P-90, Progress Report, "Development of Plutonium-Bearing Fuel Materials", p. 31.

Table 2.2

Summary of Preparation Data
for Coprecipitated UO_2-5 w/o PuO_2

Sample Identification	871-A-3A & B	297-Pu-14A	297-Pu-14B
Precipitation Conditions Method Temperature, °C	 Continuous 60	 Continuous 58	 Continuous 58
Feed Composition gm Pu/liter gm U/liter H+, molarity	 5.25 100.00 1.0	 5.41 100.30 1.0	 5.41 100.30 1.0
Feed Flow Rate, liters/hr	1.20	1.25	1.25
Precipitant Composition NH_4OH, molarity	14.8	14.8	14.8
Precipitant Flow Rate liters/hr	0.20	0.25	0.25
Precipitation Average Holdup, minutes	32	30	30
Total No. of Throughputs	8.5	3.8	3.8
Drying Temperature, °C	200	200	200
Furnace Conversion Conditions Reduction Temperature, °C Reduction Time, minutes Gas Atmosphere	 740 ± 5 100 N_2-6% H_2	 740 ± 5 85 N_2-6% H_2	 740 ± 5 85 N_2-6% H_2

Table 2.3

Effect of Hammermilling on Powder Characteristics
Coprecipitated UO_2-5 w/o PuO_2

Sample Number	Milling Treatment	B.E.T. Surface Area M^2/gm	Bulk Density gm/cc	Tap Density gm/cc	Air Permeability Particle Size microns	Average MSA Particle Size for 1200 mesh Fraction, microns	w/o Greater Than 74μ (200 mesh)
871-A-3A NM	None	6.1	1.48	1.63	4.8	0.35	66
871-A-3A HM	Hammermilled	6.1	0.76	1.72	0.45	0.72	10
871-A-3B NM	None	5.8	1.22	1.47	2.3	0.45	56
871-A-3B HM	Hammermilled	7.1	0.62	1.45	0.39	1.00	8

Table 2.4

Seemingly Anomalous Effect of Reduction History on Powder Characteristics
Coprecipitated UO_2-5 w/o PuO_2

Sample Designation	Reduction History	Bulk Density (gm/cc)	Tap Density (gm/cc)	Air Permeability Avg Particle Size, microns	B.E.T. Surface Area (M^2/gm)
297-Pu-14A	740°C (70 min) + 640°C (70 min)	-	-	-	7.30
297-Pu-14A-35	740°C (70 min) + 640°C (70 min) + 740°C (35 min)	-	-	-	6.40
297-Pu-14A-780	Above + 780°C (35 min)	1.19	1.70	0.6	6.23
297-Pu-14A-860	Above + 860°C (35 min)	1.27	1.60	3.3	6.24
297-Pu-14A-70	740°C (70 min) + 640°C (70 min) + 740°C (70 min)	-	-	-	6.30
297-Pu-14A-820	Above + 820°C (35 min)	1.21	1.68	1.4	6.00
297-Pu-14A-780 (RR)	Above + 780°C (oxidation) + 780°C (70 min)	1.45	1.72	3.9	4.62
297-Pu-14A-900	740°C (70 min) + 640°C (70 min) + 900°C (35 min)	1.19	1.58	1.4	6.4

Twin-shell blending followed by hammermilling was found to produce an unsatisfactory product since the individual powders tended to ball up; hence, the product was grossly non-homogeneous. On the other hand, wet ball milling yielded a product that could not be differentiated from coprecipitated materials after sintering these results and the techniques utilized to measure homogeneity are more fully described under Task 3.00.

In preliminary trials, individual UO_2 and PuO_2 component powders in the required amounts were each synthesized and pre-conditioned by dry-blending and hammermilling together material from near-duplicate preparation lots. The powder characteristics of the homogenized component materials (Samples BRU-1HM and BR Pu-1HM) are listed in Table 2.5 as are the characteristics following blending as described below. The surface areas of the UO_2 and PuO_2 were closely matched; however, no attempt was made to simultaneously match bulk properties or particle size. The particle size distributions for the component powders are shown in Figure 2.3. After weighing, the PuO_2 powder and an equal amount of UO_2 were pre-mixed for two hours in a PK twin-shell blender. The balance of the UO_2 was then added and blending was continued for an additional ten hours. After blending, the mixtures were samples, analyzed, and characterized (Figure 2.4). Comparison of blend particle sizes with the theoretical values predicted from data on the component powders indicates a slight growth in size. Use of an aggressive dispersion method (ultrasonic) prior to measurement would probably have eliminated this observed effect.

Analyses for plutonium were carried out by the normal amperometric titration procedure using sample quantities of 50 to 390 milligrams representing four spot samples and one composite sample from each blend. Sample-to-sample variations on plutonium content were relatively high (± 4 to 23%) indicating that segregation had occurred during blending. These data were consistent with the significant amount of "balling" or agglomeration observed during blending. In fact, tap and bulk density measurements on the component PuO_2 powder (Table 2.5) show that a significant amount of agglomeration had occurred prior to blending with UO_2.

Subsequent treatment showed that these PuO_2 agglomerates created during the original two-hour blending step also survive hammermilling treatment, despite the use of extremely fine (0.010 in) slotted herringbone screens. Also, complete dispersion of these agglomerates was not accomplished by one pass hammermilling in a Bantam Micro Pulverizer or by subsequent dry-pressing. Eventually, it was found that wet ballmilling under standard conditions for four hours yielded a satisfactory product as indicated by autoradiography of the sintered pellets (see Task 3.00).

Preparation and Characterization of High Density Granular Oxide Powders
(A. Biancheria, G. Ehrlich, J. Goodman, J. Miles)

Several methods have been under development for the direct preparation of dense granular UO_2-PuO_2 and PuO_2 materials for use in the fabrication of

Table 2.5

Characteristics of Component and Dry-Blended Uranium and Plutonium Dioxide Powders

Sample	Bulk Density (gm/cc)	Tap Density (gm/cc)	Surface Area (M^2/gm)	Air Permeability Particle Size microns	Average M.S.A. Particle Size microns	Per Cent Less Than 74 microns
UO_2 BR-U-1 (blended 2 hrs)	1.68	2.03	4.05	4.4		
UO_2-BR-U-1 HM (hammermilled)	0.76	1.87	4.12	0.50	0.64	98
PuO_2 BR-Pu-1 (blended 2 hrs)	2.23		4.0	3.3		
PuO_2 BR-Pu-1 HM (hammermilled)	1.85	3.56	4.45	1.2	3.0	98
UO_2-5 w/o PuO_2 MB-R5 (blended 12 hrs)*	2.48	2.85	4.33	2.32	0.6	98
UO_2-20 w/o PuO_2 MB-R-20 (blended 12 hrs)*	2.30	3.12	4.27	1.12	0.8	98

* PuO_2 blended with equal amount of UO_2 for 2 hrs; balance of UO_2 added, and mixed for additional 10 hrs (2-qt twin-shell PK blender)

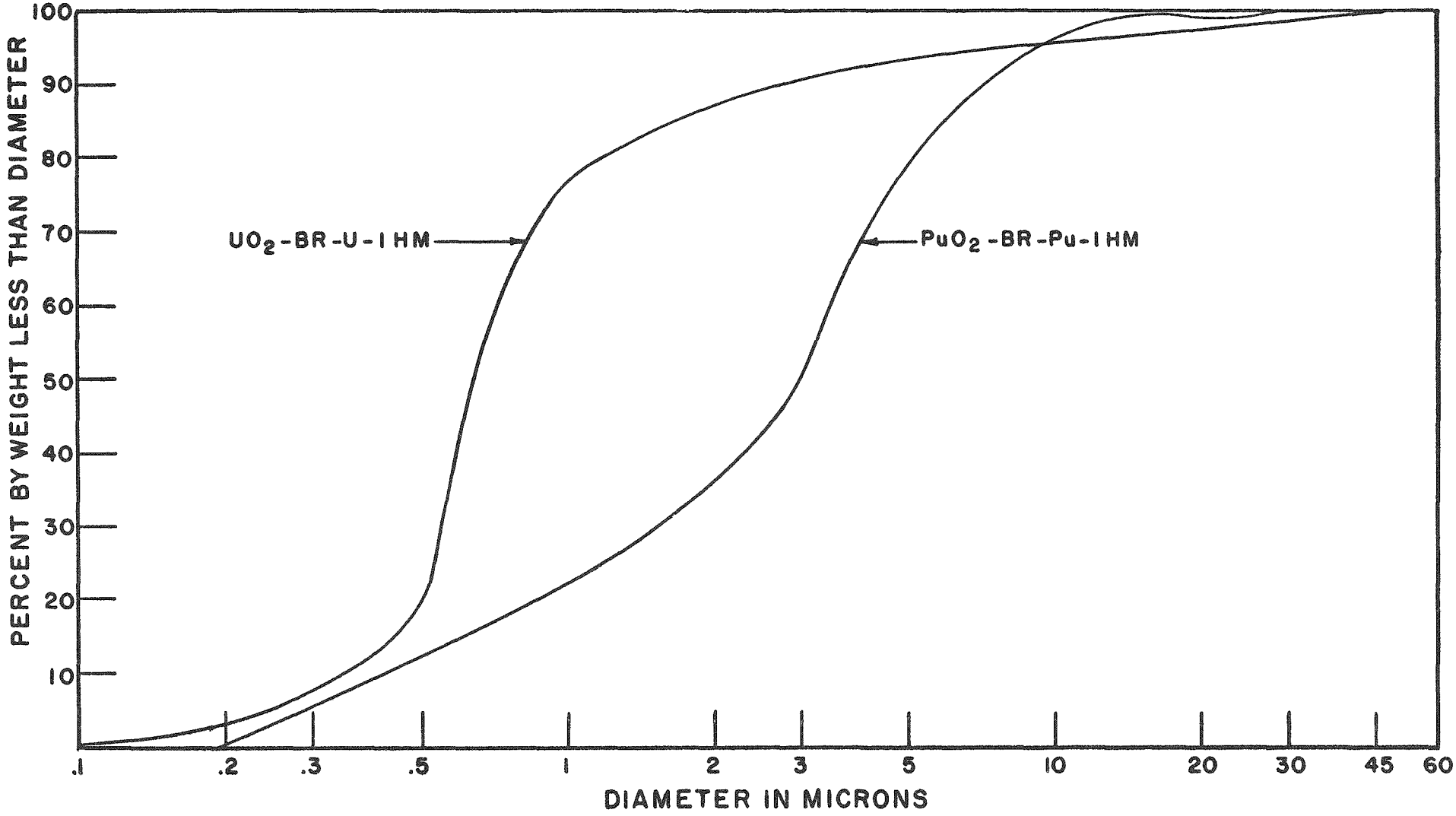

NUMEC P-100

Figure 2.3

PARTICLE SIZE DISTRIBUTIONS
OF COMPONENT PuO_2 AND UO_2 POWDERS PRIOR TO BLENDING
(M.S.A. LIQUID SEDIMENTATION METHOD)

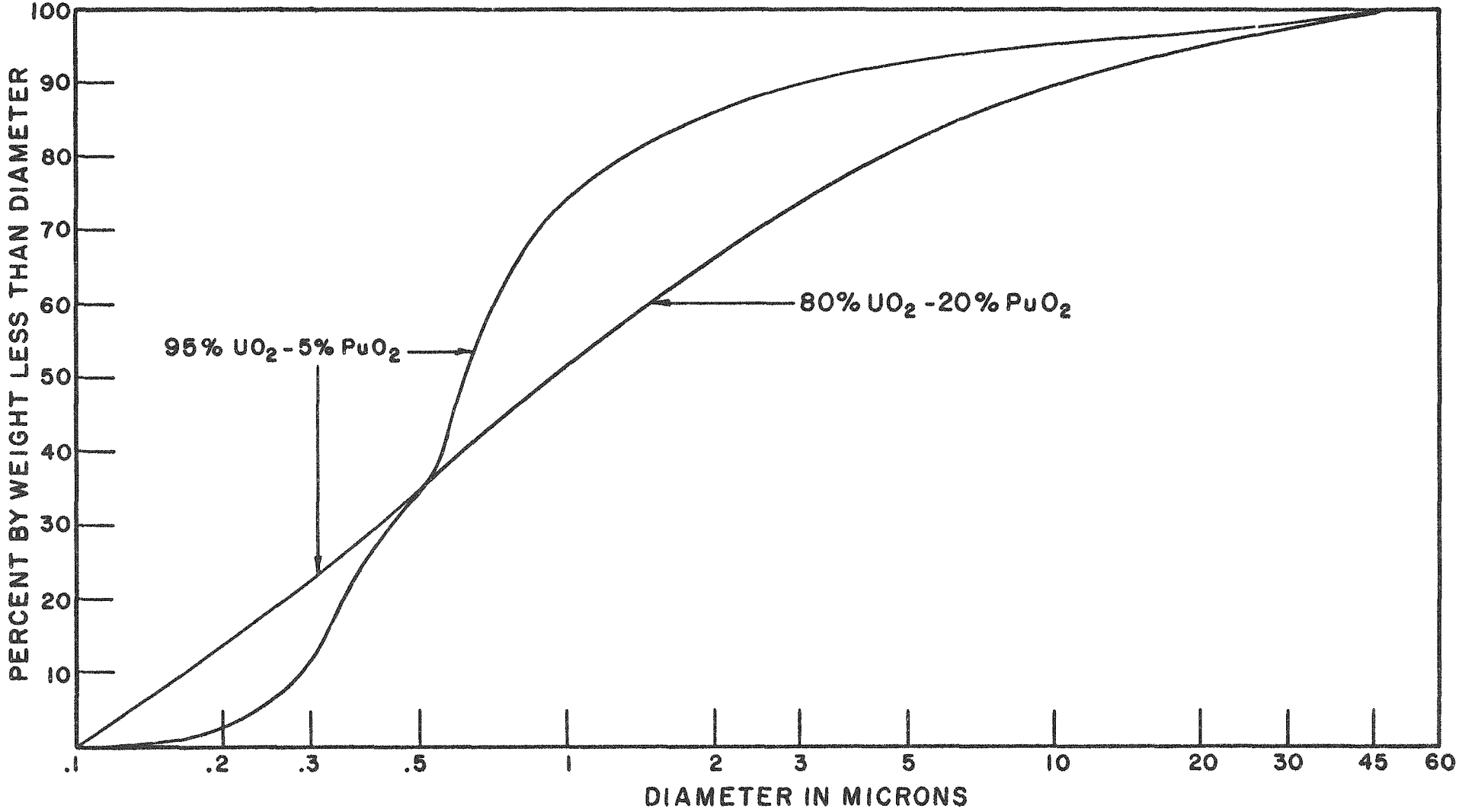

Figure 2.4

PARTICLE SIZE DISTRIBUTIONS
OF DRY-BLENDED UO_2-5% PuO_2 AND UO_2-20% PuO_2 POWDERS
(M.S.A. LIQUID SEDIMENTATION METHOD)

fuel shapes by mechanical compaction, swaging, or rolling. In addition, this type of precipitation process may also provide satisfactory feed for plasma-torch spheroidization or high surface area granular feed for pelletizing and sintering[1]. As an alternate to mechanical agglomeration of ceramic-grade powders as a forming step, precipitation of granular agglomerates may prove to be a high yield controllable process which is more suitable for plutonium-bearing materials, particularly recycled plutonium.

During this reporting period, prototype data has been obtained for a continuous precipitation process utilizing uranyl peroxide and plutonium peroxide intermediates. Work has also been continued on the preparation of granular materials via homogeneous (urea) precipitation and via the uranyl oxalate route.

Preparation of powders containing PuO_2 will commence shortly, utilizing information obtained from these prototype experiments.

Peroxide Precipitation Route

The preparation of uranyl peroxide was carried out continuously in a reactor provided with a stirrer by the simultaneous slow addition of uranyl nitrate and dilute hydrogen peroxide solutions with continuous slurry withdrawal to maintain constant volume. Processing conditions and partial product characterization data are presented in Table 2.6. A photomicrograph of a typical peroxide material (1462) is shown in Figure 2.5. The powder is seen to consist of individual particles, the majority of which are almost spherical in shape. Measured particle diameters are within the 40-80 micron range. UO_2 prepared from these peroxide precursors by reduction at temperatures of 740, 850, and 900 C had surface areas of 1.29, 0.65, and 0.79 M^2/gm. The densification of these products with further heat treatment at elevated temperatures is currently being examined. Additional studies relating the effects of preparation variables with physical properties and ease of densification are planned for the near future.

Homogeneous Precipitation from Uranyl Nitrate Solutions Using Urea

Processing conditions for four uranyl nitrate-urea runs have been presented earlier[ii]. Similar data for three additional preparations are presented in Tables 2.7 and 2.8. Two of these preparations (60-17-32 and 60-32-1) were carried out on a relatively large scale.

(i) N. Schönberg, U. Runfors, R. Kiessling, Proc. 2nd United Conf. on Peaceful Uses of Atomic Energy, Vol. 6, pp. 624-629 (1958).

(ii) NUMEC P-80, Progress Report, "Development of Plutonium-Bearing Fuel Materials", p. 29.

Table 2.6

Uranium Peroxide Processing Data

Run Number	1461	1462	1463
Uranium conc., gm/l	70.0	70.0	70.0
Vol of U feed, l	1000	1000	1000
Uranium flow rate, ml/min	6.1	2.5	4.2
H_2O_2 conc, gm/l	44	44	100
Vol of H_2O_2 feed, l	1425	1360	1400
H_2O_2 flow rate, ml/min	8.6	3.4	5.8
Reactor vol, l	400	400	400
Residence time, min	27	68	40
No. of throughputs	6	6	6
Reaction temp, °C	24	24	24
U conc, filtrate, gm/l	0.209	0.013	0.006
Reduction atmosphere	N_2-6% H_2	N_2-6% H_2	N_2-6% H_2
Rate of temp rise, °C/min	30	30	30
Reduction temp, °C	900	850	740
Reduction time (plateau), min	60	120	45
Surface area of UO_2, M^2/gm	0.79	0.65	1.29
Bulk density, gm/cc	2.2	-	-
Tap density, gm/cc	3.2	-	-
Sub-sieve size, microns	4.6	-	-

Table 2.7

Reaction Conditions
for Uranyl Nitrate-Urea Homogeneous Precipitation

Experiment Number	60-17-32	60-29-9	60-32-1
Source of uranium	Eldorado ADU	Eldorado ADU	Eldorado ADU
Weight of material taken	262.5	87.2	262.5
Moles UO_2^{2+}	0.75	0.25	0.75
Initial volume of UO_2^{2+} solution, ml	1050	350	1050
Moles urea taken	2.25	.75	2.25
Initial volume of urea solution, ml	420	150	450
Additional time of urea solution, min	10	2	10
Total final volume of solution, ml	1470	500	1500
Urea/UO_2^{2+}	3	3	3
Reaction temperature	Reflux	Reflux	Reflux
Reaction time, hrs	18	22	23
Drying conditions			
Temperature, °C	60	25	25
Atmosphere	Air	Air	Air
Time, hrs	18	100	200
Weight of dried ADU, gm	250.0	86.6	237.8

Table 2.8

Conversion Conditions
for Preparation of UO_2 from ADU

Run Number	60-17-32	60-29-9
Weight of material charged, gm	250.0	86.6
Gas composition	N_2-6% H_2	N_2-6% H_2
Gas flow rate, cfm	4	4
Rate of temp. climb, °C/min	4	6.5
Conversion temperature, °C	740	840
Time at temperature, min	85	60
Weight of product, gm	212.6	58.2
% conversion	85.4	83.0
O/U ratio	2.31	2.10
Surface area, M^2/gm	3.03	7.86

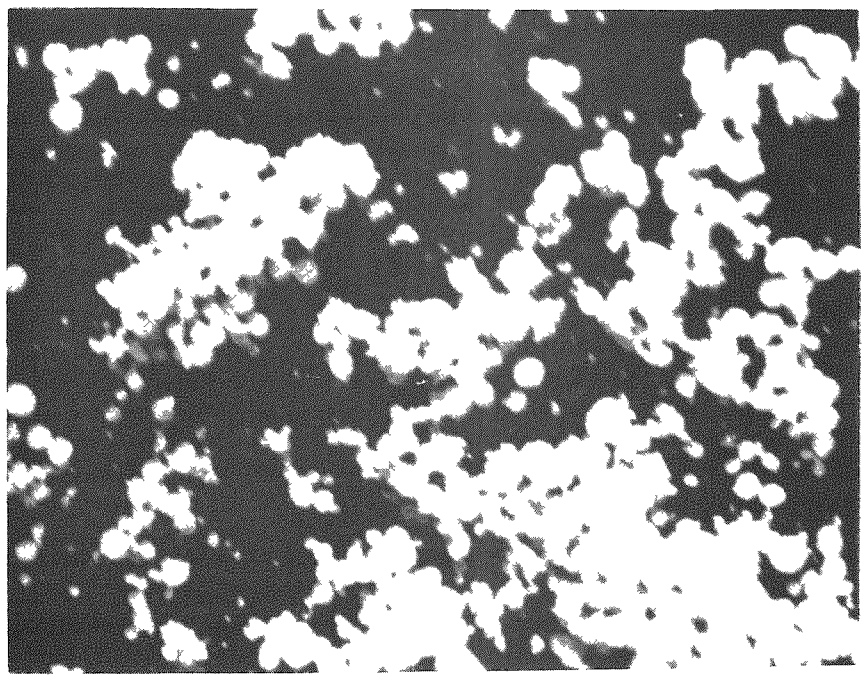

Figure 2.5

Photomicrograph of Granular Uranyl Peroxide
Sample No. 1462

80X

As before, the granular yellow intermediate powders appeared to be composed of individual spheroidal particles. Photomicrographs of this intermediate product (60-29-9) and the derived UO_2 are shown in Figures 2.6 and 2.7. It is seen that the spheroidal shape persists through the conversion process from the intermediate compound to the UO_2 with only slight diminution of particle size.

Electron micrographs of specimens from the previously prepared sample (1405) show small arrowhead shaped particles. Two typical electron micrographs are shown in Figure 2.8. Close microscopic examination reveals a sandstone structure with the presence of many small holes in the particle surface. Determinations of particle density are being carried out at the present time to assist in interpretation.

Uranyl Oxalate Preparation Route

Some additional uranyl oxalate preparations have also been made. Processing conditions are shown in Table 2.9. The crystalline yellow uranyl oxalate powder was prepared over a wide range of conditions of temperature, precipitating reagent, solvent, and reaction time. Photomicrographs of specimens of each preparation were obtained. In general there was a wide variation in crystal size and shape from preparation to preparation, but all products exhibited evidence of nearly complete crystallization. A photomicrograph of a typical oxalate specimen (60-9-18) is shown in Figure 2.9.

Several samples of typical uranyl oxalate preparations were converted to UO_2 under conditions presented in Table 2.10. Corresponding product characterization data are also presented in this Table.

The results suggest that small variations in the wet processing method have less effect upon the final UO_2 characteristics than do the conditions under which the uranyl oxalate is converted to UO_2. A number of additional uranyl oxalate preparations are now in progress to provide a more complete understanding of the process.

Photomicrographs of two specimens of UO_2 derived from 60-9-18 uranyl oxalate are shown in Figure 2.10. It is noted that the external shape of the particles corresponds closely to the external shape of the oxalate precursor. This effect was noted earlier in the conversion of the urea hydrolysis intermediate to UO_2. Microscopic examination of the surface of the UO_2 derived from uranyl oxalate fails to reveal any evidence of unusual pore structure although many fissures are visible.

Analytical Chemistry

(O. Menis, E. Halteman, E. Garcia, P. Rey, and R. Jaroszeski)

The study of the application of x-ray emission and gamma spectrometry to the analyses of preparations of mixed oxides of uranium and plutonium has

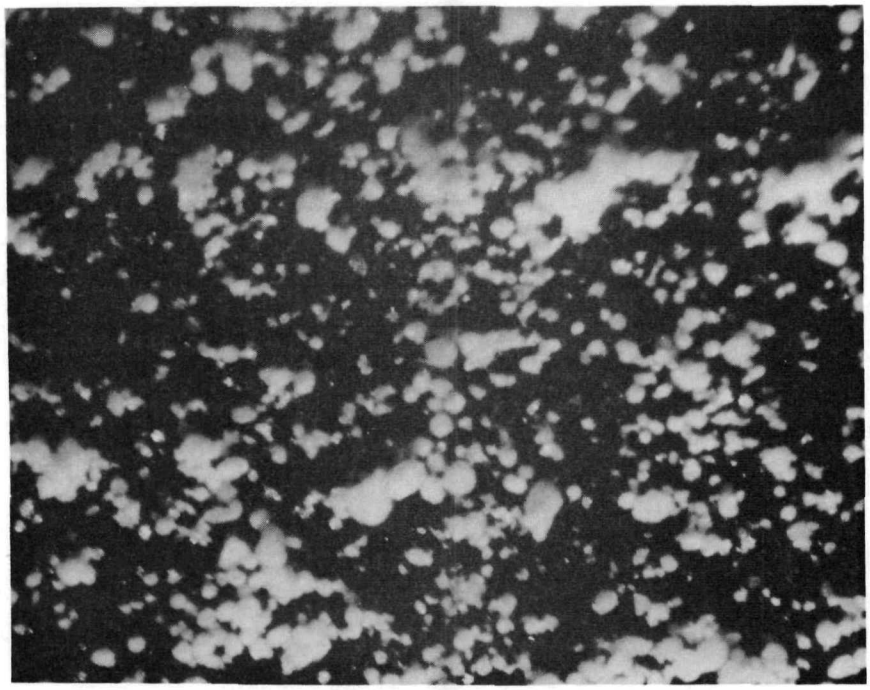

Figure 2.6
Photomicrograph of Granular Intermediate Precipitate from Uranyl Nitrate-Urea Homogeneous Precipitation
Sample 60-29-9 80X

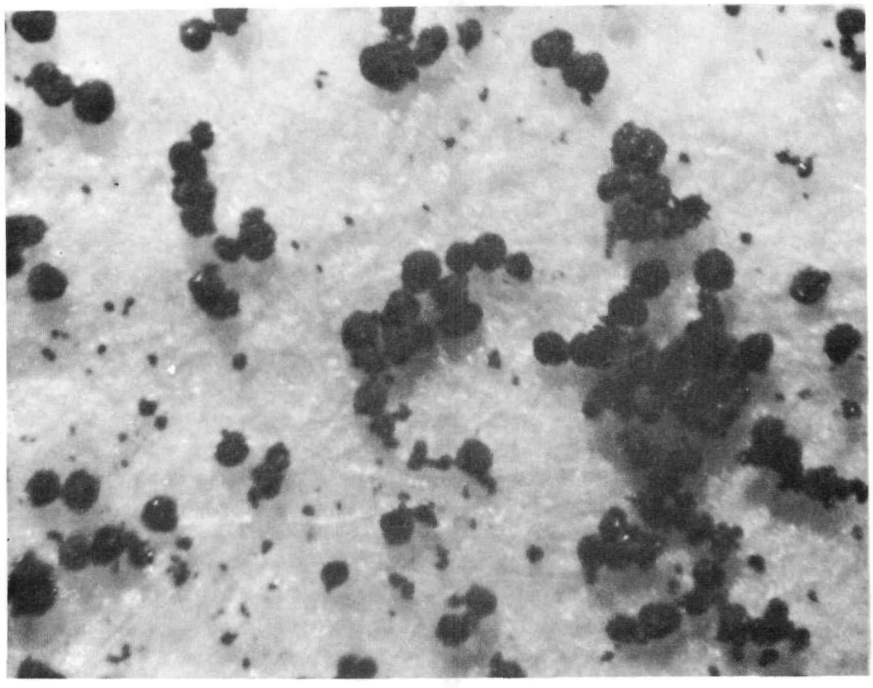

Figure 2.7
Photomicrograph of Granular UO_2 from Homogeneous Precipitation
Sample 60-29-9 80X

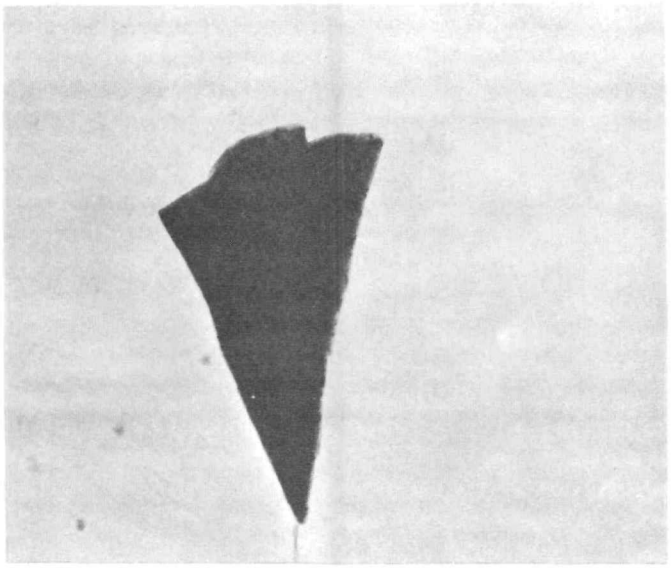

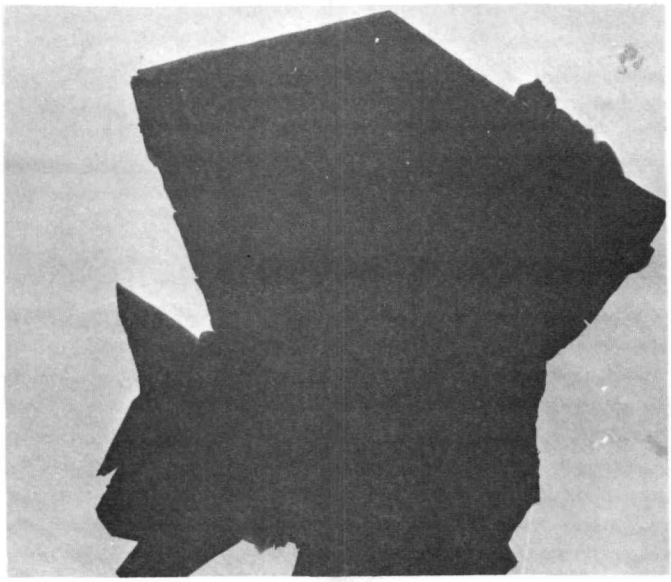

Figure 2.8

Electron Micrographs of Intermediate Compound Prepared by Uranyl Nitrate-Urea Precipitation

(Sample No. 1405)

12,000X

Table 2.9

Reaction Conditions for Precipitation of Uranyl Oxalate Granular Crystals

Experiment Number	19-4-8	60-4-14	60-4-26	60-5-23	60-5-35	60-9-18	60-10-1
Source of uranium	UNH*	UNH	UNH	UNH	UNH	UNH	UNH
Solvent	H_2O + HNO_3 pH = 1	H_2O	50 vol % EtOH 50 vol % H_2O	H_2O	H_2O	H_2O	H_2O
Moles $[UO_2]^{++}$	0.25	0.125	0.062	0.125	0.062	0.125	0.062
Initial volume of $[UO_2]^{++}$ solution, ml	500	483	250	350	240	350	240
Source of $[C_2O_4]^{=}$ ions	$H_2C_4O_4$***	Et_2OX**	Et_2OX	H_2OX	Et_2OX	H_2OX	Et_2OX
Moles $[C_2O_4]^{=}$	0.75	0.125	0.066	0.125	0.066	0.125	0.066
Initial volume of $[C_2O_4]^{=}$ solution, ml	100	17	9	150	9	150	9
Additional time of $[C_2O_4]^{=}$ solution, ml	2	5	2	2	2	2	2
Total final volume of solution, ml	600	500	259	500	249	500	249
$[C_2O_4]^{=}$/ UO_2^{++}	3	1	1.06	1	1.06	1	1.06
Temperature, °C	Reflux	Reflux	Reflux	(5 hrs at 95	25	Reflux	(44 hrs at 25**
Reaction time, hrs	1	18½	18½	(64 hrs at 25	68	40	(30 hrs at 95
Drying Conditions							
Temperature, °C	90	80	80	50	50	25	25
Atmosphere	Air	Vac	Vac	Vac	Vac	Vac over P_2O_5	Vac over P_2O_5
Time, hrs	2	18	18	18	18	18	18
Weight of dried precipitate, gm	-	42.9	21.6	42.5	22.3	39.2	17.0
% U in precipitate****	-	61.2	62.9	60.3	59.8	-	-
Yield on U basis	-	88	92	86	91	-	-

* Supplied by Eldorado Mining and Refining
** Eastman #123 - White Label Diethyl Oxalate
*** Baker and Adamson #1141 - Oxalic Acid, crystal, reagent, ACS
**** Product heated in air at 900°C for 2 hours. % U calculated on basis of U_3O_8 produced from a given weight of product.

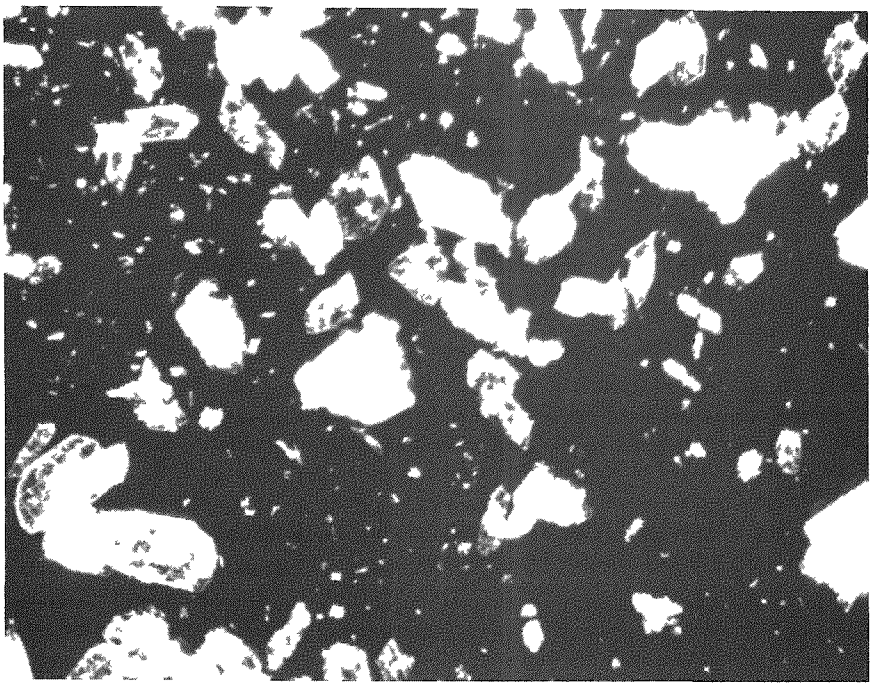

Figure 2.9

Photomicrograph of Uranyl Oxalate

Sample No. 60-9-18 28X

Table 2.10

UO_2 Conversion Conditions
for Uranyl Oxalate Preparations
and Product Characterization Data

Run Number	60-4-14	60-4-14	60-5-23	60-5-23	60-9-18	60-9-18
Weight of charge, gm	15.00	15.00	15.00	15.00	15.00	15.00
Gas composition	N_2-6% H_2	N_2-6% H_2	N_2-6% H_2	N_2-6% H_2	N_2-6% H_2	N_2-6% H_2
Flow rate, ft^3/hr	4	4	4	4	4	4
Rate of heat up, ^oC/min	15	30	15	30	15	30
Conversion temp, ^oC	540	740	540	740	540	740
Time at temp, min	45	45	45	45	45	45
Weight of product, gm	10.65	10.52	9.79	10.55	10.16	10.05
% conversion	65.2	70.3	65.7	70.5	68.7	66.8
O/U Ratio	2.23	2.11	2.23	2.12	2.25	2.13
Surface area, M^2/gm	10.4	5.1	13.8	4.7	9.9	4.7
Bulk density, gm/cc	0.75	0.75	0.93	0.90	0.93	1.01
Tap density, gm/cc	1.34	1.86	1.59	1.86	1.63	1.82
Sub-sieve size, microns	2.07	-	1.96	-	1.95	-

Sample 60-9-18 40X

Sample 60-9-18-740 40X

Figure 2.10

Photomicrographs of UO_2
Derived from Uranyl Oxalate

been continued. Calibration curves have been generated for specific specimens and conditions. Further work is necessary to simplify sample preparation and to increase accuracy.

X-ray Emission Analysis

Chemical analysis by x-ray emission is of particular interest since it can serve as verification of the accuracy of the analyses of major components by the spectrophotometric procedure[i]. Further, it has the advantage over the spectrophotometric method in that it is relatively free of interference from impurities or additives. Also, this method should make it feasible to obtain a more accurate value for the uranium content in preparations which have a relatively high percentage of plutonium.

X-ray emission studies have been reported in the literature for the determination of plutonium in solutions[ii] and in slurries[iii]. In the development and adoption of these procedures to the mixed oxides, several variables are being investigated to optimize precision and accuracy. The areas being studies include the selection of appropriate internal standards, the effect of various fluxes or diluents, the effect of variation in composition, and the methods for suitable sample preparation.

A Philips Norelco Universal X-ray Spectrograph, Model 52360, with its associated components is being used for this work. The components include a lithium fluoride crystal (2d = 4.0276Å); a tungsten target x-ray tube, type FA-60; a scintillation counter, type 52245; a pulse height analyzer, type 52332; and a scaler, type 421455.

A number of standard samples have been prepared with different amounts of contained PuO_2 and an internal standard, ThO_2. The PuO_2 was prepared by calcination of high purity metal and the ThO_2 was reagent grade material. Known quantities of the oxides were weighed into a 50 ml beaker and fused at 450°C with 10 grams of potassium pyrosulfate. The selection of potassium pyrosulfate as flux was based on previous experience[iv][v]. This medium

---

(i) NUMEC P-70, Progress Report, "Development of Plutonium-Bearing Fuel Materials", p. 23.

(ii) D. S. Flikkema and R. V. Shablaske, USAEC Report AN-5804 (1957).

(iii) W. S. Turnley, Talanta 6, 189 (1960).

(iv) NUMEC P-70, Progress Report, "Development of Plutonium-Bearing Fuel Materials", p. 18.

(v) T. J. Cullen, Anal. Chem. 32, 516 (1960).

effectively dissolves the refractory mixed oxides and at the same time serves as good diluent with low absorption properties.

The fusion was carried out for a period of approximately four hours until, on visual examination of the melt, a transparent solution was achieved. The fused mass was then poured into a teflon tray and allowed to cool, after which it was ground in an agate mortar to approximately 200 mesh size. The powder was then pressed at 9000 psi to obtain briquettes $1\frac{1}{4}$ inch in diameter and approximately $\frac{1}{2}$ inch thick.

By measurement on both sides of the briquette, it was occasionally found that some segregation had occurred at the surface. In those cases where significant differences were noted, surface polishing eliminated the discrepancy. Studies are now under way with other flux materials which could provide a solid bead, hence, eliminate the need for briquette pressing and grinding.

Each briquette was loaded into a sample holder having a mylar window. The intensity of the emission was measured at five different angles, three of them, 24.12, 26.62, and 29.12°, for background correction, and two, 24.89 and 27.46, for the plutonium and thorium emission peaks. A fixed time technique was chosen to collect approximately a total of 20,000 counts at the plutonium and thorium peaks. Typical data suitable for calibration are presented in Table 2.11.

The calibration curve based on these data is not linear over the entire range of Pu/Th weight ratios. The reasons for deviation from linearity are discussed in the literature[(i)(ii)]. The higher slope with increasing amounts of plutonium can be attributed to the self-absorption effect. Despite this non-linearity, good reproducibility is attainable with the use of a calibration curve. The relative standard deviation for samples containing over 15 mg of plutonium in the presence of high concentrations of diverse ions (Co, Ni, Cr, Mo, W, Fe), such as found in Haynes alloy, was less than 0.6%; with 3-5 mg of plutonium in the same material, the standard deviation was less than 1%.

Determination of Plutonium by Gamma Spectrometry

The application of gamma counting for the determination of plutonium in solutions has been extended to solid samples. Similar work has been recently reported by the British[(iii)]. For this purpose, the higher energy peak at 210 kev, from the U-237 daughter of Pu-241, was chosen.

(i) H. A. Liebhafsky, H. G. Pfeiffer, W. H. Winslow, and P. D. Zemany, "X-Ray Absorption and Emission in Analytical Chemistry", John Wiley & Son, Inc., New York (1960).

(ii) J. Cope, Norelco Reporter 3, 41 (1956).

(iii) A. J. Fudge, G. Philip, E. Foster, "Non-Destructive Determination of Plutonium-239 in Ceramic Fuel Element Pellets by Gamma Spectrometry", AERE-R 3838, Sept. 1961.

Table 2.11

Calibration Date for Plutonium by X-ray Emission

Standard Number	Pu/Th Weight Ratio	Counts/Minute at Angle ⊖					Background Correction cpm		Net Counts cpm		Pu/Th Intensity Ratio	Intensity Ratio
		24.12°	24.89°	26.62°	27.46°	29.12°	24.89°	27.46°	Pu	Th		Weight Ratio
1	0.044	1183	1181	973	2381	739	1112	887	69	1494	0.046	1.045
2	0.059	1162	1191	952	2524	728	1092	866	100	1658	0.060	1.017
3	0.201	1167	1306	964	1872	740	1100	879	206	993	0.207	1.030
4	0.556	1187	1750	974	1875	757	1115	892	635	983	0.646	1.162
5	0.803	1180	2040	971	1857	753	1110	888	930	970	0.959	1.194
6	1.156	1135	2440	952	1853	741	1072	872	1368	981	1.394	1.206

Two techniques were investigated; one, the application of a calibration curve and the other a standard addition procedure. The results of the calibration method are presented in Table 2.12 and Figure 2.11. In the region 0.8 to 2 mg of Pu, the results are fairly linear with relative standard deviation of less than 5%. For solid samples which contained large concentrations of absorbing material, a standard addition technique permitted analysis without the need for duplication of conditions for calibration purposes.

Future studies aimed at improving precision will include measurement at the 384 kev peak.

Table 2.12

Determination of Plutonium by Gamma Spectrometry
(Data for a Typical Calibration Curve)

Sample Number	Total Pu mg	cpm	cpm/mg Pu
1	10.3	734	71.3
2	1.91	183	95.8
3	1.34	123	91.8
4	0.84	74	88.1

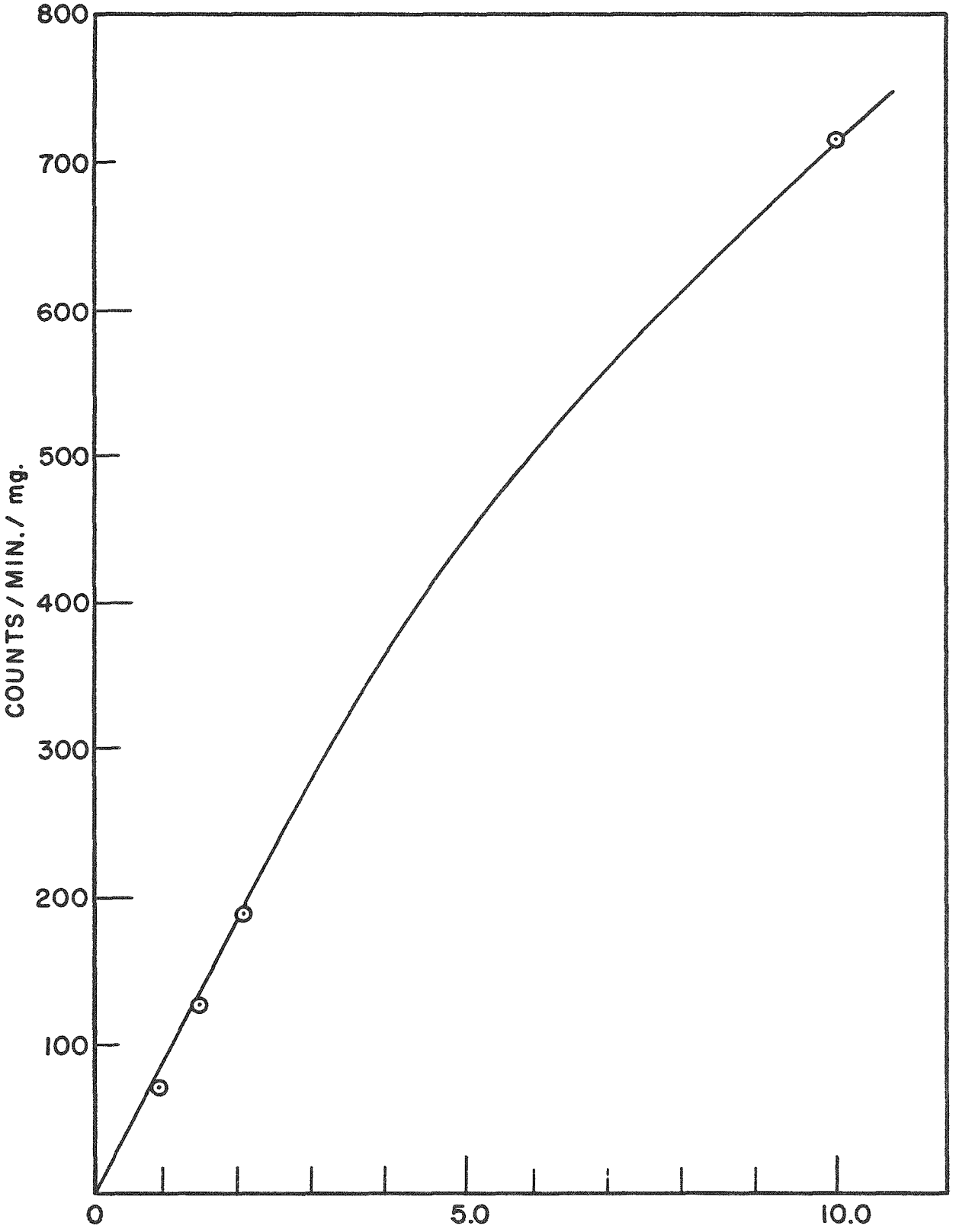

Figure 2.11

DETERMINATION OF PLUTONIUM BY GAMMA SPECTROMETRY

MEASUREMENT AT THE 214 Kev ENERGY PEAK

FABRICATION AND EVALUATION OF FUEL SHAPES

Task 3.00

E. K. Halteman L. J. Jones

Mixed Oxide Sintering Studies

(M. D. Houston)

Investigation of the fabrication parameters for UO_2-5 w/o PuO_2 and UO_2-0.5 w/o PuO_2 by the cold compaction and sintering method has been continued. The feed material was produced by coprecipitation, uranium as ammonium diuranate and plutonium as plutonium hydroxide, and subsequent reduction to the oxides at 750°C in nitrogen-6% hydrogen. It has previously been shown that this reduction cycle results in formation of a solid solution of the oxides. The resultant powders were prepared for compaction by hammermilling, slug pressing, and granulation through a 35 mesh screen. All pellets were dry pressed using only a Sterotex die lubricant. During this period, approximately 600 grams of UO_2-5 w/o PuO_2 and 50 grams of UO_2-0.5 w/o PuO_2 have been processed. The sintering furnace impurities previously observed(i) have been analyzed and corrective action taken. Previous difficulties experienced with the sintering of mixed oxide pellets have been attributed to the presence of these furnace impurities.

It was reported in the previous progress report that a significant number (approximately 15%) of UO_2-5 w/o PuO_2 pellets were fractured or coated with a glassy substance during the firing cycle. Observed at the fractured interfaces were foreign inclusions or areas of apparent fusion. A crystalline growth was also noted both in the sintering furnace tube and on the molybdenum boat. These needlelike crystals were analyzed by x-ray fluorescence, x-ray diffraction, and emission spectrographic techniques. Since the main constituents were found to be molybdenum and silicon, it was postulated that an intermetallic compound of these two elements might be present as the impurity. However, the diffraction pattern did not agree with published data for any of the molybdenum silicides. Trace quantities of iron, nickel, uranium, and plutonium were also found in the needles. Analysis of a sample taken from the cold zone of the furnace showed the presence of cadmium, boron, manganese, gallium, and lead. Subsequent spectrographic analysis of the furnace components (wire, tube, grain, and cement) showed that these components were free of the offending high cross section elements. It has now been established that these elements were present in significant amounts in the as-received plutonium nitrate and thereby built up in the furnace

---

(i) NUMEC P-90, Progress Report, "Development of Plutonium-Bearing Fuel Materials", page 54.

over a period of time. This problem is now being discussed with the plutonium supplier. The sintering furnace has been cleaned of all loose powdery material, and molybdenum sintering boat covers are now being used to minimize furnace contamination. Approximately 40 pellets of UO_2-5 w/o PuO_2, which were fired in this protected manner, showed no evidence of fracturing or of "glass" formation. Crystalline material was still found on the boat handle but was prevented from contacting the pellets.

Sintering data for the coprecipitated UO_2-5 w/o PuO_2 and UO_2-0.5 w/o PuO_2 material are presented in Table 3.1. These data show that sintered densities are not greatly influenced by the PuO_2 concentration or the processing variables (compacting pressure, firing time, firing temperature) in the ranges studied. As expected, slight improvements in the green density with increasing compaction pressure and fired density with increasing firing time and temperature were found. Good reproducibility is also illustrated by the results.

The processing of fired scrap material from fractured or imperfect pellets was continued. An oxidation-reduction cycle of four hours at 1000°C in air followed by four hours at 800°C in nitrogen-6% hydrogen was utilized to break down the sintered particles. The sintering characteristics of this reworked material indicated that the cycling was not beneficial in producing high density pellets. The densities of pellets produced from material given one, two, and three such cycles was 8.53, 8.17, and 7.06 gm/cc, resp. A density of 9.40 gm/cc had been obtained under identical sintering conditions from the fired material as crushed and rehammermilled. During the progressive oxidation-reduction cycles, the resultant material took on a reddish hue which might indicate the formation of U_3O_8; this could explain the low densities observed. Oxygen analyses are being made to verify this postulate.

PuO_2 Sintering Studies

(M. D. Houston, J. Miles)

The sintering characteristics of PuO_2 have been examined by evaluating different oxide preparations, compaction pressures, and firing time, temperature, and atmosphere.

Two lots of PuO_2 powder prepared by the oxalate route and calcined in air at 760°C were used. Sample 297-Pu-9-3, which was used for the major portion of this investigation, had a surface area of 4.1 M^2/gm while Sample 297-Pu-9-4 measured 7.5 M^2/gm. A considerable difference in the sintering characteristics of these two lots can be seen in the data presented in Table 3.2. The higher surface area material produced the higher fired density, as expected.

The studies made to determine the effort of compaction pressure indicate that compaction pressure has little, if any, effect upon the final fired

Table 3.1

Sintering Data for Coprecipitated UO_2-PuO_2 Compacts

Composition	Compaction Pressure(1) (TSI)	Green Density (gm/cc)	Firing Time (hrs)	Firing Temp(2) (°C)	Fired Density (gm/cc)	Theoretical Density(3) %	Linear Shrinkage (%)
UO_2-0.5 w/o PuO_2	8	5.04	1	1550	10.22	93.2	21.4
	8	5.00	2	1550	10.32	94.1	21.8
	9	5.11	1	1550	10.23	93.3	21.0
	9	5.14	2	1550	10.34	94.3	21.1
	10	5.19	1	1550	10.12	92.3	20.4
	10	5.20	2	1550	10.36	94.5	20.8
	8	5.05	1	1600	10.38	94.7	21.6
	8	5.01	2	1600	10.42	95.0	22.0
	9	5.13	1	1600	10.41	94.9	21.3
	9	5.12	2	1600	-	-	21.3
	10	5.18	1	1600	10.31	94.0	20.8
	10	5.14	2	1600	10.35	94.4	21.2
	8	5.03	1	1650	10.40	94.8	21.8
	8	5.06	2	1650	10.42	95.0	21.7
	9	5.12	1	1650	10.37	94.6	21.4
	9	5.15	2	1650	10.44	95.2	21.3
	10	5.18	1	1650	10.40	94.8	21.1
	10	5.17	2	1650	10.35	94.4	21.0
UO_2-5 w/o PuO_2							
Lot A1	8	4.87	1	1600	10.39	94.5	22.0
Lot A2	8	4.97	1	1600	10.42	94.8	21.5
Lot A3	8	4.89	1	1600	10.50	95.5	23.8

(1) Slugged at 5 TSI and granulated through 35 mesh.
(2) All samples fired in 94% nitrogen-6% hydrogen.
(3) Theoretical density of UO_2-0.5 w/o PuO_2 - 10.97 gm/cc.
Theoretical density of UO_2-5 w/o PuO_2 - 10.99 gm/cc.

Table 3.2

Sintering Studies for PuO_2
Compacting Pressure - Sintering Temperature - Sintering Atmosphere

Lot	Compaction Pressure (TSI)	Green Density (gm/cc)	Firing Time (hrs)	Firing Temperature (°C)	Firing Atmosphere	Fired Density (gm/cc)	Theoretical Density (%)	Linear Shrinkage (%)
Pu-9-3	7.3	6.28	1	1600	N_2/H_2	9.97	87.0	13.9
(Compaction	18.1	6.94	1	1600	(94:6)	10.12	88.2	11.1
Pressure)	28.9	7.30	1	1600	(94:6)	10.19	88.8	8.9
	37.9	7.56	1	1600	(94:6)	10.10	88.1	7.7
	45.2	7.68	1	1600	(94:6)	10.12	88.2	7.3
Pu-9-3	31.5	7.22	1	1200	N_2/H_2	10.03	87.5	10.2
(Firing	31.5	7.32	1	1300	(94:6)	10.21	89.1	10.1
Temperature)	31.5	7.36	1	1400	(94:6)	10.31	90.0	10.0
	31.5	7.37	1	1500	(94:6)	10.33	90.1	10.3
	31.5	7.36	1	1600	(94:6)	10.16	88.6	9.4
Pu-9-3	31.5	7.37	1	1500	N_2/H_2	10.33	90.1	10.3
(Firing	31.5	7.34	1	1550	Air	10.46	91.2	10.5
Atmosphere)	31.5	7.34	1	1550	Air	10.51	91.7	10.8
Pu-9-4	19.7	6.79	2	1500	N_2/H_2	10.58	92.2	14.1
(Firing	41.4	7.29	2	1500	N_2/H_2	10.59	92.3	10.7
Atmosphere)	31.5	7.16	1	1550	Air	10.90	95.1	17.2
Pu-9-3	7.9	6.28	1	1600	N_2/H_2	9.97	87.0	13.9
(Firing	8.2	6.18	4	1600	(94:6)	9.96	86.9	14.8
Time)	7.3	6.18	16	1600	(94:6)	9.75	85.1	14.4
	41.4	7.55	20	1600	(94:6)	10.01	87.4	8.7
	8.2	6.42	72	1600	(94:6)	10.23	89.3	14.9

density under the sintering conditions studied. However, microstructural differences which followed a pressure relationship were noted. Considerable porosity was observed in the lower pressure compacts (7-19 T/in^2), while in the higher pressure compacts, the porosity was not apparent but the grain size was reduced. Photomicrographs of the pressure study compacts are shown in Figure 3.1. It is seen that the high porosity and large grain size of the lower pressure specimens changes to low porosity and small grain size in the higher pressure specimens. Also, in the lower pressure compacts, dark bands of a second phase, presumably Pu_2O_3, can be seen. These bands are not apparent in the higher pressure compacts even though Pu_2O_3 was detected by x-ray examination.

The results relating fired density to firing temperature, other factors being constant, indicate that a temperature in the range of 1400 to 1500 °C is best for the attainment of highest density in the reducing atmosphere utilized. This confirms the earlier results(i). The reduced density and linear shrinkage observed after 1600°C firing may be attributed to the partial reduction of PuO_2 to Pu_2O_3.

The results also show that the fired density is not particularly dependent upon the firing time at temperature in the range considered.

The results relating to the effect of sintering atmosphere indicate that higher densities are attainable by firing in air rather than in N_2-H_2. This is to be expected since PuO_2 is the highest oxide of plutonium and Pu_2O_3 has a much lower physical density (10.2 gm/cc). Further investigations of the efforts of compaction pressure and firing temperature within the limits of the furnace with air atmosphere will be undertaken.

The pellets sintered in nitrogen-6% hydrogen and utilized in the previously described compaction pressure study subsequently were re-oxidized in air at 1000°C for 16 hours. The results are shown in Table 3.3. It is to be noted that the weight gains due to air exposure were far below the values anticipated from previous results. This indicates that the amount of Pu_2O_3 existing in these pellets before reoxidation was only 9-13% compared to 25-30% measured previously in other samples. These data were verified since no additional weight gain was noted following subsequent comminution of the pellets and refiring in air at 1000°C for four hours. From the trend of decreased Pu_2O_3 formation with increasing compaction pressure, it can be postulated that the degree of Pu_2O_3 formation is determined by the surface area available during the early stages of the sintering process.

(i) NUMEC P-70, Progress Report, "Development of Plutonium-Bearing Fuel Materials", page 36.

Table 3.3

Reoxidation of PuO_2
1000°C - 16 Hours - Air

Lot	Compacting Pressure	Fired Density gm/cc	Weight Loss on Firing mg/gm	Weight Gain on Reoxidation mg/gm	Calculated Amount of Pu_2O_3 %
Pu-9-3	7.3	9.84	97	40.6	13.45
	18.1	10.12	91	39.9	13.20
	28.9	9.65	90	36.1	11.95
	37.9	9.98	85	31.7	10.50
	45.2	10.11	88	28.0	9.27

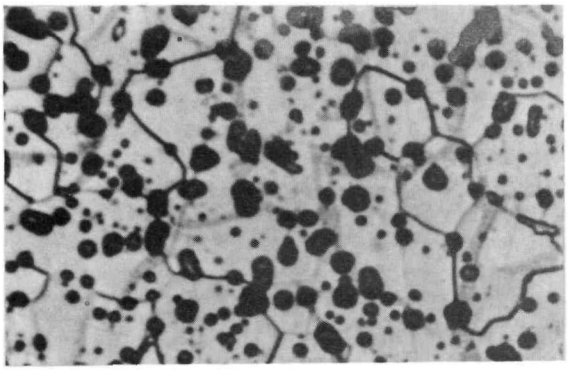

Compaction Pressure 7.25 TSI
Neg. 41B

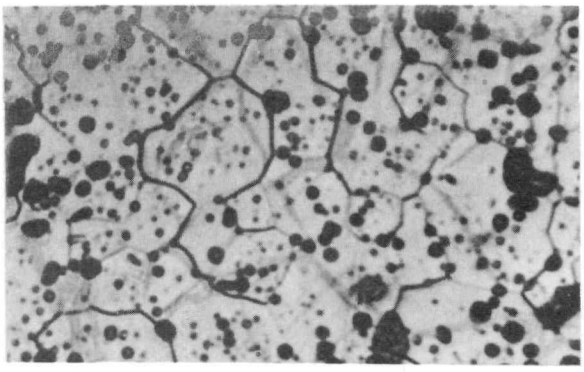

Compaction Pressure 18.05 TSI
Neg. 42B

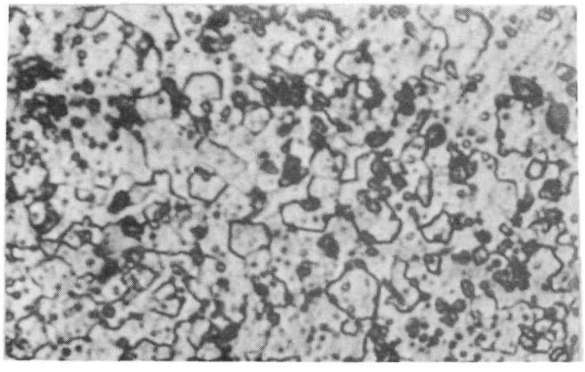

Compaction Pressure 28.90 TWI
Neg. 43B

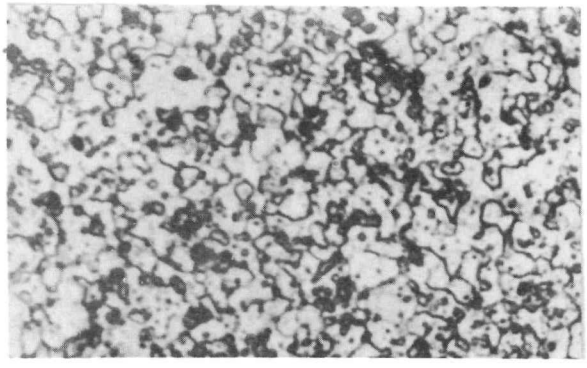

Compaction Pressure 37.90 TSI
Neg. 44B

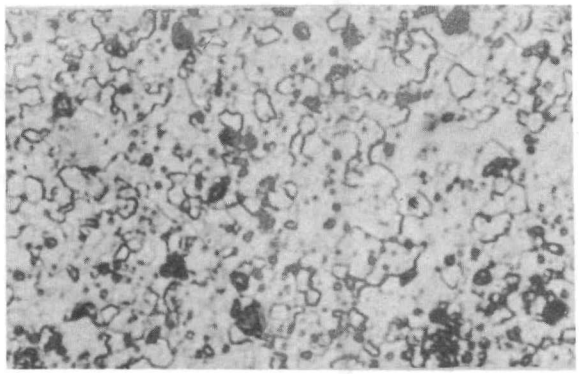

Compaction Pressure 45.15 TSI
Neg. 45B

Figure 3.1
Photomicrographs of Sintered PuO_2 Compacts
(Sintered at 1600°C for 1 hour in N_2-6% H_2)
800X

Rabbit Test Fuel Fabrication
(M. D. Houston, B. Cinai)

The fabrication of samples for short-term irradiations in hydraulic rabbit facilities is continuing. The final fired pellets have been evaluated by optical microscopy, x-ray diffraction, and autoradiography to determine adequacy of initial material blending, homogenization during firing, and sintering characteristics. Four UO_2-PuO_2 compositions have been prepared from both coprecipitated and mechanically-mixed individual compound powders. X-ray diffraction has indicated a single phase for the coprecipitated material and two distinct fluorite structures for the mechanical blends, as expected.

As discussed under Task 2.00, in preliminary trial preparations, considerable balling was noted in the mechanically mixed powders following twin-shell blending. As shown in Figure 3.2, these miniature spheres were retained in the compacted and fired pellets of these materials. Further examination by autoradiography verified this macroinhomogeneity, and more satisfactory blending techniques were, therefore, developed.

The autoradiography of the ends of the pellets was accomplished by transferring a polished metallographic section, after decontamination, out of the glove box into a special container having a double window of 0.00025 inch thick Mylar sheet. Exposure of the x-ray film by direct contact with the Mylar for approximately 45 seconds resulted in satisfactory radiographs. The autoradiograph shown in Figure 3.3 is from the identical sample shown in Figure 3.2 and shows the pronounced balling effect with multi-layered spheres of alternating UO_2-rich and PuO_2-rich layers. It is pointed out that this autoradiograph is a negative of the alpha-particle exposed x-ray film, and hence, the high alpha producing regions, i.e., high plutonium regions, appear white. As discussed under Task 2.00, this balling effect occurs during the initial stages of blending of the very fine UO_2 and PuO_2 powders. It is to be noted that these spheres remain intact through the pre-slugging at 5 TSI, the manual granulation, and the cold compaction at 8-10 TSI. Further treatment by hammermilling of the powders after blending resulted in the nonhomogeneous fragments shown in Figure 3.4. Subsequent wet ball milling of the blended powders gave a uniform textured mixture and pellet as shown in Figure 3.5. For comparison, an autoradiograph of a UO_2-20% PuO_2 pellet made from coprecipitated powder is shown in Figure 3.6. It can be seen that the wet ball milling results in material which has a macrohomogeneity similar to coprecipitated material. Therefore, this processing has been adopted for all mechanically mixed compositions for the irradiation specimens.

The compaction and sintering characteristics of the various UO_2-PuO_2 compositions to be used for the rabbit irradiations and also for UO_2 and PuO_2 are given in Table 3.4. In general, the mechanically blended materials yielded lower densities and shrinkages than the coprecipitated batches. Most of this behavior is probably due to the sequential formation

Table 3.4

Compaction and Sintering Data for Oxide Pellets
(Sintered at 1600°C in N_2-6% H_2 Atmosphere)

Composition	Preparation	Compaction Pressure (TSI)	Green Density (gm/cc)	Firing Time (hrs)	Fired Density (gm/cc)	Theoretical Density (%)	Linear Shrinkage (%)
UO_2	ADU	8.2	5.15	4	10.41	95.0	21.3
	ADU	8.2	5.09	16	10.52	96.0	21.8
	ADU	8.2	5.18	20	10.56	96.3	21.3
UO_2-5% PuO_2 (w/o)	Mechanical Blend (MB)	8.2	5.19	4	10.32	94.0	20.6
	MB	8.2	5.23	16	10.52	95.8	20.9
	MB + Ball Mill	8.2	5.14	16	10.59	96.4	21.2
	MB + Ball Mill	8.2	5.45	20	10.36	94.2	20.1
	Coprecipitated	8.2	5.04	4	10.63	96.8	22.3
	Slugged and Granulated	9.1	5.11	16	10.60	96.5	21.9
	Slugged and Granulated	8.2	4.9	20	10.52	95.8	22.8
	(Not slugged)	8.2	4.88	72	10.49	95.5	23.1
UO_2-20% PuO_2	MB	8.2	5.33	4	10.36	93.6	19.9
	MB	7.8	5.28	16	10.41	94.1	20.4
	MB + Ball Mill	8.2	5.30	16	10.64	96.1	20.2
	MB + Ball Mill	8.2	5.69	20	10.16	91.8	17.5
	Coprecipitated	8.2	4.91	4	10.70	96.7	23.1
	Slugged and Granulated	11.2	5.09	16	10.73	97.0	22.3
	Slugged and Granulated	8.2	5.14	20	10.68	96.5	22.0
	(Not slugged)	8.2	4.74	72	10.53	95.1	23.9
PuO_2	Oxalate	8.2	6.18	4	9.96	86.9	14.8
	Oxalate	7.3	6.18	16	9.75	85.0	14.4
	Oxalate	41.4	7.55	20	10.01	87.5	8.7
	Oxalate	8.2	6.42	72	10.23	89.3	14.9

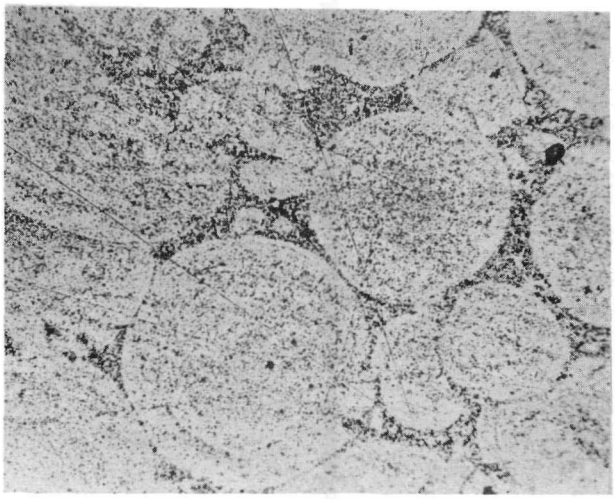

Figure 3.2

Photomicrograph of Sintered Pellet
of Mechanically Blended UO_2-20 w/o PuO_2
(Sintered at 1600°C for 4 hours in N_2-6% H_2)

100X
Neg. 249

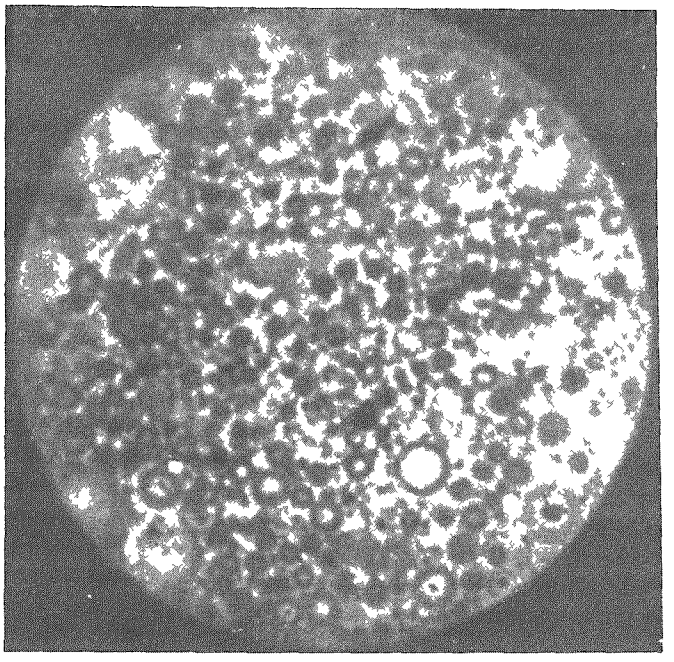

Figure 3.3
Autoradiograph of Sintered Pellet
of Mechanically Blended UO_2-20 w/o PuO_2
(Sintered at 1600°C for 4 hours in N_2-6% H_2)
Neg. 11 13.5X

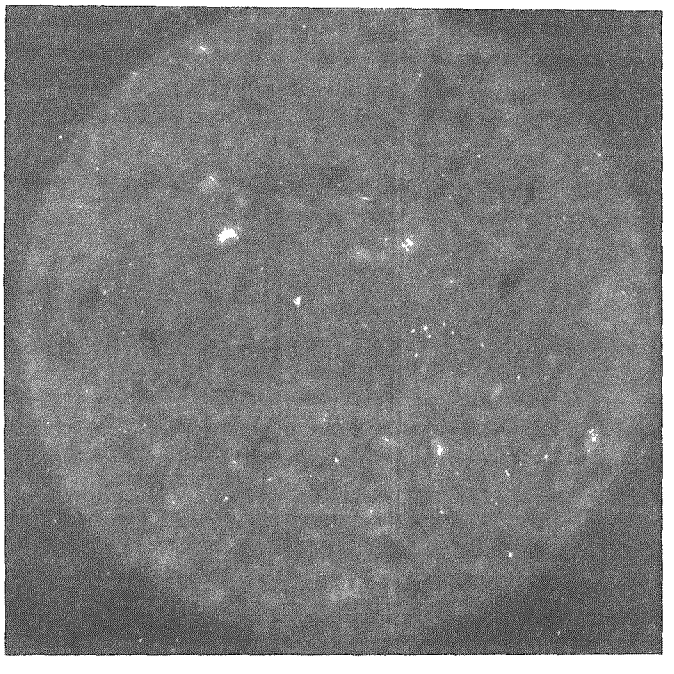

Figure 3.4
Autoradiograph of Sintered Pellet
Mechanically Blended and Hammermilled UO_2-20 w/o PuO_2
(Sintered at 1600°C for 16 hours in N_2-6% H_2)
Neg. 19 13.5X

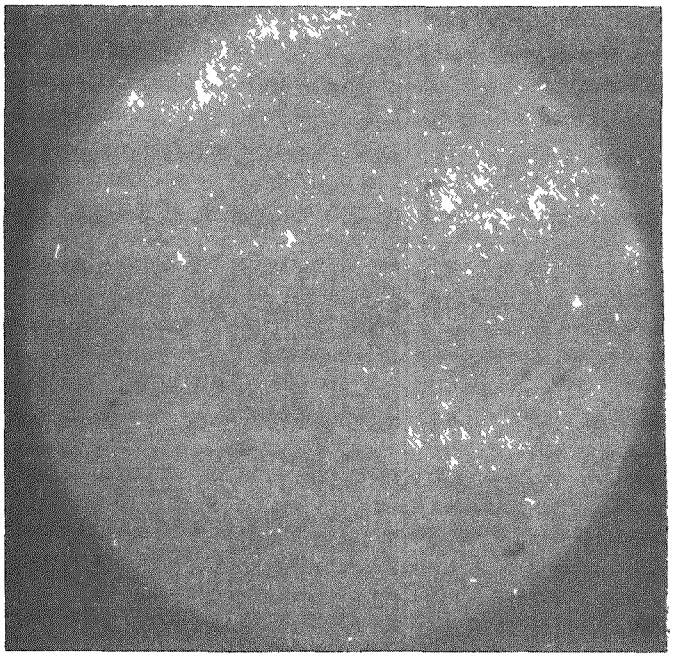

Figure 3.5

Autoradiograph of Sintered Pellet
of Mechanically Blended and Wet Ball Milled UO_2-20 w/o PuO_2
(Sintered at 1600°C for 16 hours in N_2-6% H_2)
Neg. 18 13.5X

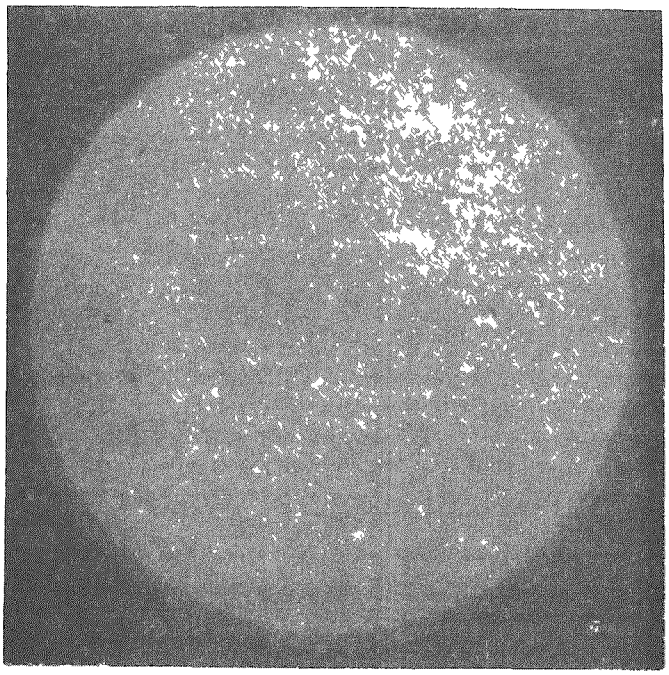

Figure 3.6

Autoradiograph of Sintered Pellet
of Coprecipitated and Co-reduced UO_2-20 w/o PuO_2
(Sintered at 1600°C for 16 hours in N_2-6% H_2)
Neg. 20 13.5X

of solid solution, i.e., either before or during sintering. Also, a slight effect may be due to the low surface area of the PuO_2 used, 297-Pu-9-3 having a surface area of 4.1 M^2/gm. It is also to be noted that fired densities for the coprecipitated materials are slightly higher than for pure UO_2. All densities except those for PuO_2, which is not required for the irradiation tests, were equivalent to or better than the specified requirements for the irradiation samples. X-ray diffraction patterns indicate that single phase material resulted from the 5 w/o and 20 w/o PuO_2 batches which had been mechanically blended, ball milled, and fired. Two phases, PuO_2 and Pu_2O_3, were found to be present in the pure PuO_2 pellets. However, microstructural examination of these specimens failed to show the eutectoid structure, Figures 3.7 and 3.8. The reason for this is currently under investigation. Other specimens in the series are in the preparative stage for microscopy and x-ray examinations. The longer fired samples (72 hours) were especially prepared to study possible segregation effects in the coprecipitated materials.

Thermal Conductivity Experiment
(E. K. Halteman)

The assembly of the apparatus for the measurement of the thermal conductivity of poor thermal conductors at high temperature by the use of point and plane sources is continuing. The quartz to metal seals used in the original design have been abandoned and replaced with a mechanical seal using "O" rings and a packing gland arrangement. The equipment has been assembled and made vacuum tight. The sample insertion rod mechanism has been assembled and found to work satisfactorily when under vacuum. The sample lowering rod and bottom viewing port interchange mechanism has also been made leak tight.

Work is progressing rapidly on the assembly of the auxiliary electrical equipment. The R. F. generator has been installed adjacent to the glove box. In order to improve the power transfer efficiency, the impedance matching step-down transformer has been installed inside the glove box and as close to the experiment as possible. As an initial trial, a work coil of 13 turns of flattened $\frac{1}{4}$ inch copper tubing will be used. The high voltage equipment for the electron gun is also being assembled. The high voltage filter has been tested and potted to reduce corona. This filter reduces the ripple voltage to less than 2 volts in 30 kv. An auxiliary supply of 5 kv has been assembled along with a four section LC filter. The ripple voltage of this supply is less than $1\frac{1}{4}$ volts. This power supply will be used to provide the focusing and control potentials for use with an electrostatic focusing and electrostatic deflection electron gun. With this gun the 30 kv supply will be used to provide a post acceleration potential to the electron beam.

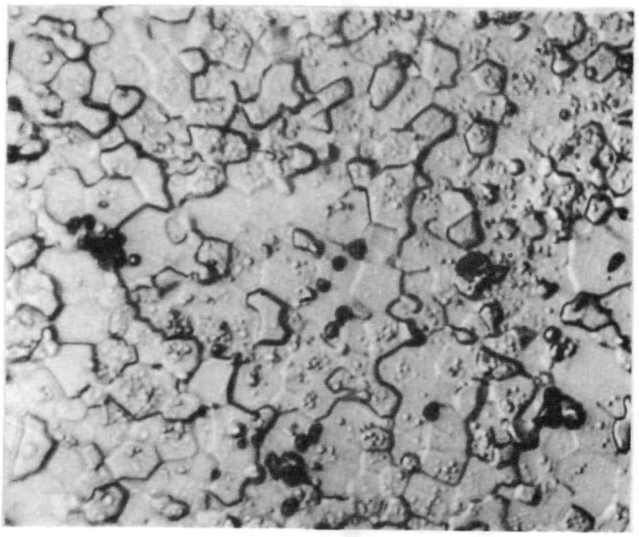

Figure 3.7

Photomicrograph of PuO_2 (297-Pu9-3)
Compacted at 8.2 TSI
(Sintered at 1600°C for 4 hours in N_2-6% H_2)
Neg. 32D 800X

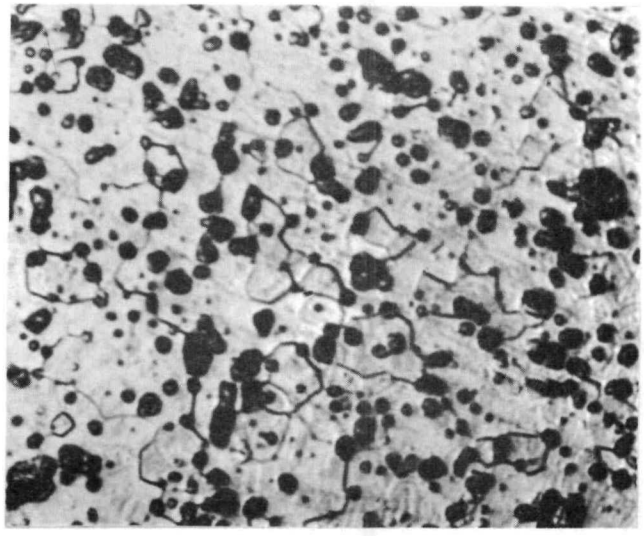

Figure 3.8

Photomicrograph of PuO_2 (297-Pu9-3)
Compacted at 7.3 TSI
(Sintered at 1600°C for 16 hours in N_2-6% H_2)
Neg. 33B 800X

FUEL ELEMENT FABRICATION AND EVALUATION

Task 4.00
L. J. Jones

Box and Equipment Installation
(M. Zambernard)

Effort is continuing on the design of glove boxes and associated equipment required for the fabrication of dispersion fuel elements by rolling. The design philosophy was presented previously(i).

Installation of the swaging machine has also been initiated. In this glove box, provisions have been made to provide a seal between the glove box end and the fuel element tube so that the length of the working piece need not be limited by glove box dimensions. This box will be tied to the transfer tunnel to allow for ready movement of material without the need for bagging.

(i) NUMEC P-90, Progress Report, "Development of Plutonium-Bearing Fuel Materials", p. 62.

RADIATION TESTING AND EVALUATION

Task 5.00
L. J. Jones

Rabbit Tests
(L. J. Jones, R. M. Horgos)

The original plans to perform the irradiation of the short-time rabbit capsules[1] in the Westinghoust Testing Reactor (WTR) have had to be discarded due to the shutting down of the WTR. The Preliminary Request for Irradiation Services (Form AEC-21) had been approved, and assignment of reactor space in the WTR had been made. Also, test specimen and capsule design had been generally approved by the WTR Project Engineering Department. Negotiations are currently under way to obtain space in another testing reactor. The irradiation facilities at these other reactors are being evaluated as to their compatibility with the proposed program. Although it is not anticipated that the fuel materials, compositions, or fuel element design will require modification, it is almost a certainty that the capsule design will require complete modification. All work associated with the capsule fabrication has therefore been stopped until reactor space has been assigned and negotiations with the assigned reactor have been initiated in regard to capsule design. Fabrication of the fuel pellets, however, has been continued as described under Task 3.00.

Hot Laboratory Equipment Fabrication
(R. M. Horgos)

Fabrication of the alpha boxes for the hot cell is continuing, and installation of remotely controlled equipment is being performed. The preliminary design of the apparatus for collecting and analyzing fission gases has been completed. Also, design of an in-cell puncturing apparatus for the fission gas studies has been initiated. For the proposed rabbit tests this puncturing apparatus will not be required since the time at temperature will be too short to allow diffusion of the fission gases out of the fuel into the fuel element can. However, this apparatus will be necessary for a complete evaluation of the fuel from the high burnup experiments which are scheduled.

The manipulators for the metallographic cell have been completely overhauled and installed in the contaminated metallographic cell. The exterior of the cell has been completely decontaminated and painted. Decontamination of the cell interior is now in progress utilizing the repaired manipulators.

(i) NUMEC P-90, Progress Report, "Development of Plutonium-Bearing Fuel Materials", pp. 63 and 64.

Construction of the in-cell alpha enclosure for the metallographic cell has been delayed pending installation of a cathodic vacuum etcher since previous results[1] indicate that such etching is for superior to normal chemical procedures.

(i) NUMEC P-90, Progress Report, "Development of Plutonium-Bearing Fuel Materials", pages 59 and 60.

REACTOR PHYSICS AND ENGINEERING PARAMETRIC STUDIES

Task 8.00
K. H. Puechl

Assessment of Plutonium Potential in Near-Thermal Reactors
(W. Ross, J. Ruzbacki)

A more detailed comparison of U-235 vs plutonium fuel cycle costs in near-thermal converter reactors has been carried out to supplement the previously reported studies[i]. In general, the plutonium isotopic composition, physics assumptions, cost assumptions, and calculation procedures were those used in the earlier study. As discussed in the last progress report, the results are not particularly sensitive to cross-section assumptions[ii]; hence, the conclusions can be considered to be generally valid.

Specifically, the object of the study was to compare optimum fuel cycle costs achievable with a plutonium-natural uranium loading to those attainable with a slightly enriched uranium loading under the assumptions that radiation damage is not limiting and that an "ideal" burnable poison (or solution poison) could be used to hold down the excess reactivity. These data, therefore, give a true comparison of ultimate potential fuel cycle costs. The analyses were performed on a Yankee-type core containing similar fuel elements and identical neutron leakage.

For each particular lattice spacing, denoted by $\xi\Sigma_s/\Sigma Ni$ (macroscopic slowing down power per heavy atom), calculations were performed at a number of different enrichments in order to determine the enrichment that results in minimum fuel cycle costs under the specific cost assumptions utilized. These optimum cost values so determined are presented in Figure 8.1. It is seen that the optimum fuel cycle cost for plutonium fueled systems is 2.205 mills/kwh and occurs at $\xi\Sigma_s/\Sigma Ni = 150$. In comparison, the optimum cost for uranium fueled systems is 2.52 mills/kwh which occurs at $\xi\Sigma_s/\Sigma Ni = 110$. In order to achieve optimum costs, a more dilute lattice is therefore indicated for plutonium. Operation under such conditions would tend to increase capital costs (since less heat could

---

(i) K. H. Puechl, "The Potential of Plutonium as a Fuel in Near-Thermal Converter Reactors", Nuclear Science and Engineering: 12, 135-150 (1962).

(ii) NUMEC P-90, Progress Report, "Development of Plutonium-Bearing Fuel Materials", p. 66.

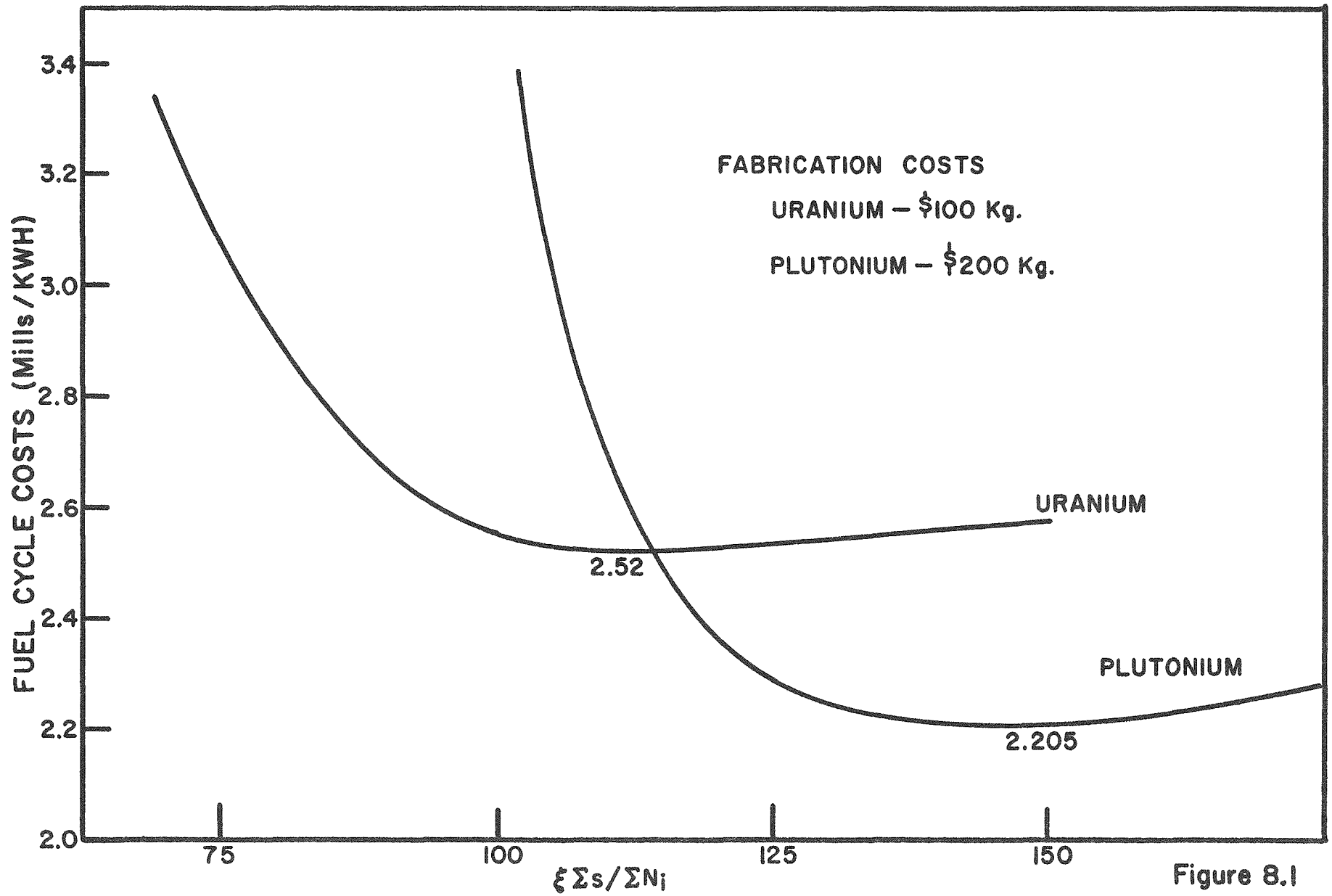

Figure 8.1

OPTIMUM FUEL CYCLE COSTS FOR PLUTONIUM–NATURAL URANIUM AND SLIGHTLY ENRICHED URANIUM FUEL LOADINGS IN NEAR–THERMAL CONVERTER REACTORS

be extracted from the same sized core); however, this seeming disadvantage can be offset by using fuel that is diluted with a low cross section material such as ZrO_2. Studies are planned to determine the effect of such dilution, and if the results so indicate, to initiate experimental investigation of materials preparation.

Figures 8.2 and 8.3 are presented to illustrate the details behind the cost data presented in Figure 8.1. It is seen that to achieve the optimum fuel costs for both uranium and plutonium loadings requires irradiation to an average of 30,000-40,000 MWD/Tonne. Such core lives are not now feasible with present fuel materials technology. However, if calculations indicate merit to dilution of plutonium with ZrO_2 to increase power density, then a by-product advantage of increased irradiation stability due to the addition of this inert material may be considered.

Figure 8.4 shows the associated initial hot, equilibrium fission product reactivities for these optimized fuel cycle cost loadings. It is seen that the amount of reactivity that must be controlled for uranium systems is appreciably greater than for corresponding plutonium systems. The shimming needed for plutonium systems can be controlled by rods while a burnable poison or solution poison would be a necessity for the uranium loadings.

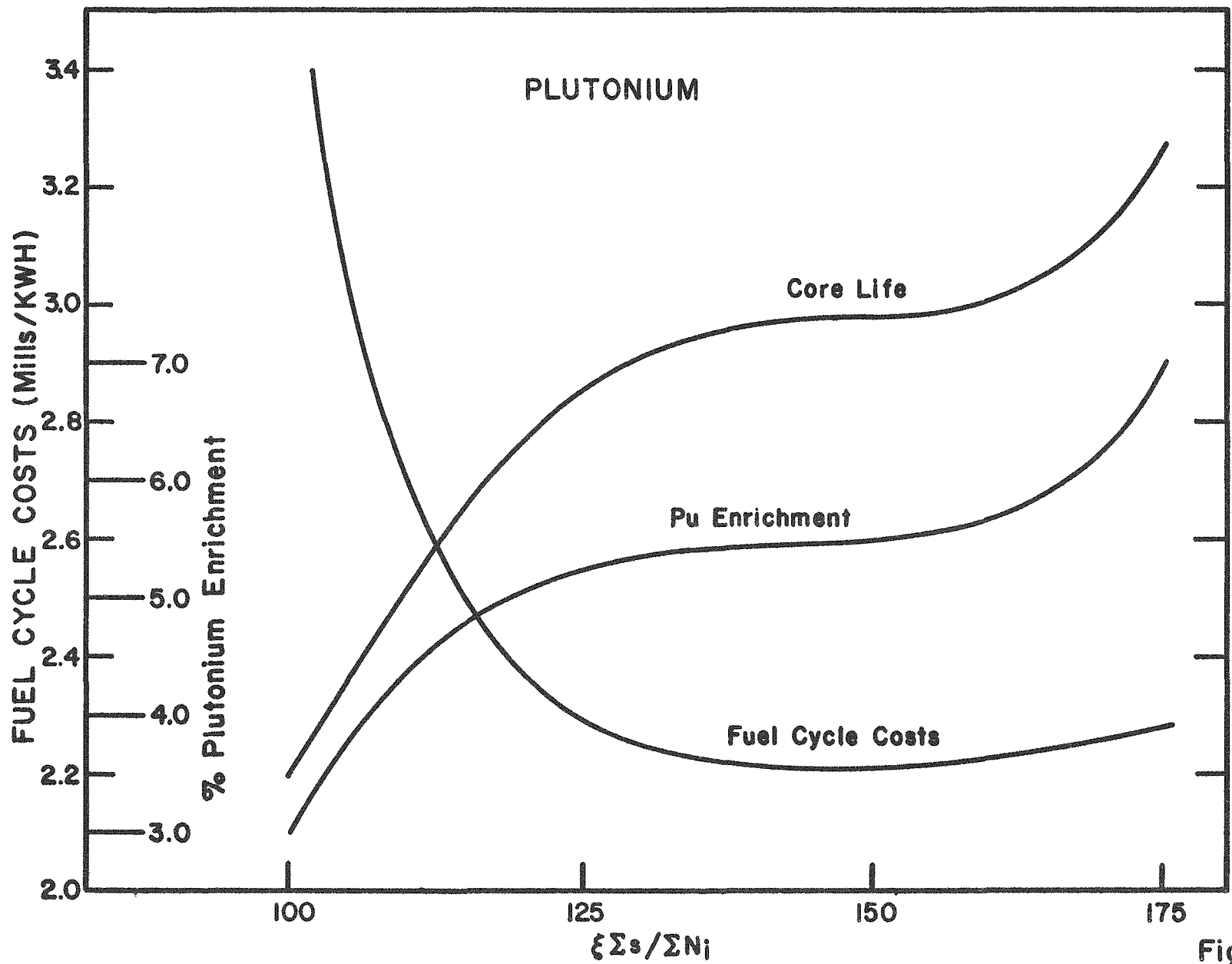

NUREG P-100

Figure 8.2

PLUTONIUM VARIATION OF CORE LIFE AND ENRICHMENT WITH OPTIMUM FUEL CYCLE COSTS FOR DIFFERENT DEGREES OF MODERATION

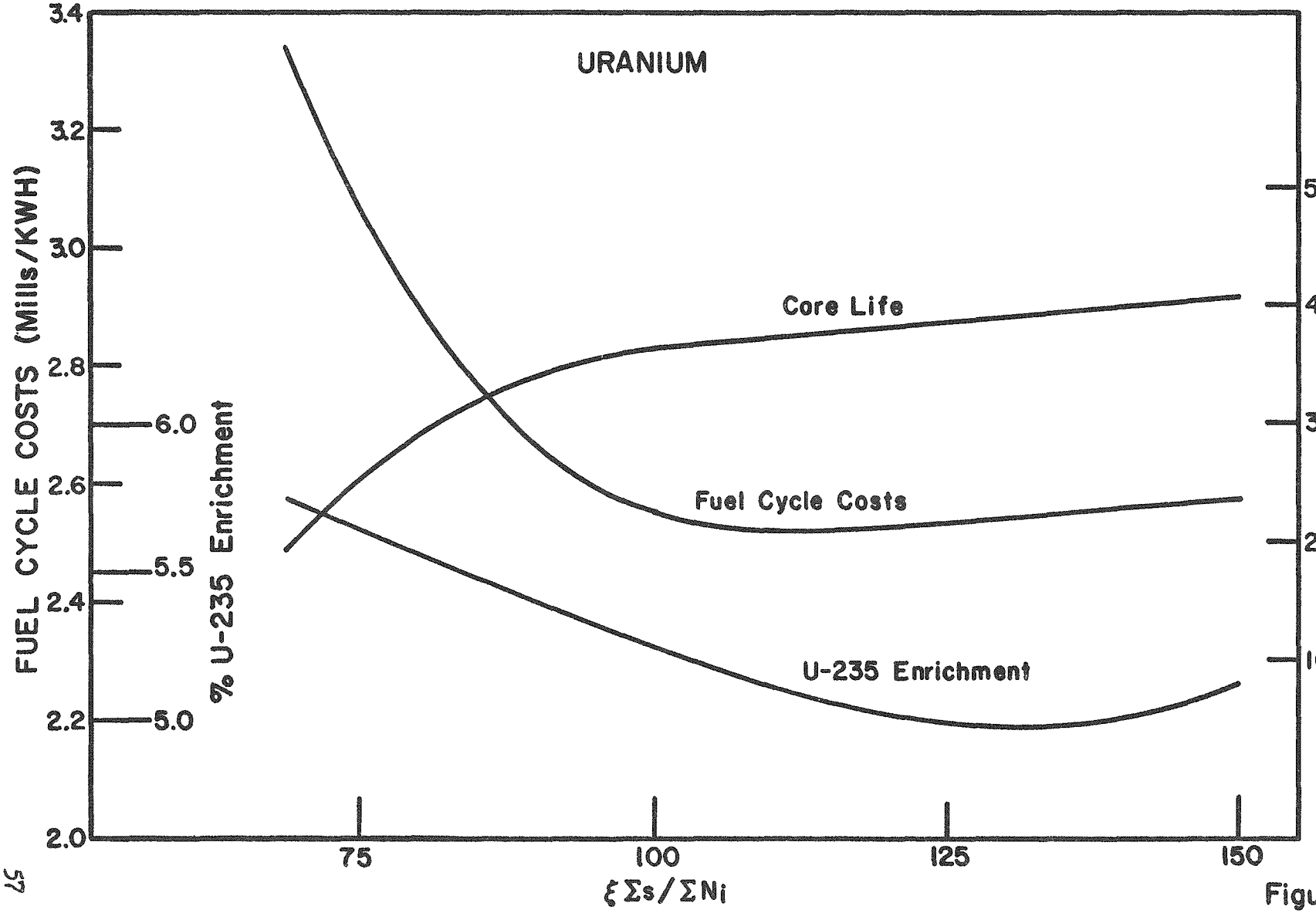

Figure 8.3

URANIUM VARIATION OF CORE LIFE AND ENRICHMENT WITH OPTIMUM FUEL CYCLE COSTS FOR DIFFERENT DEGREES OF MODERATION

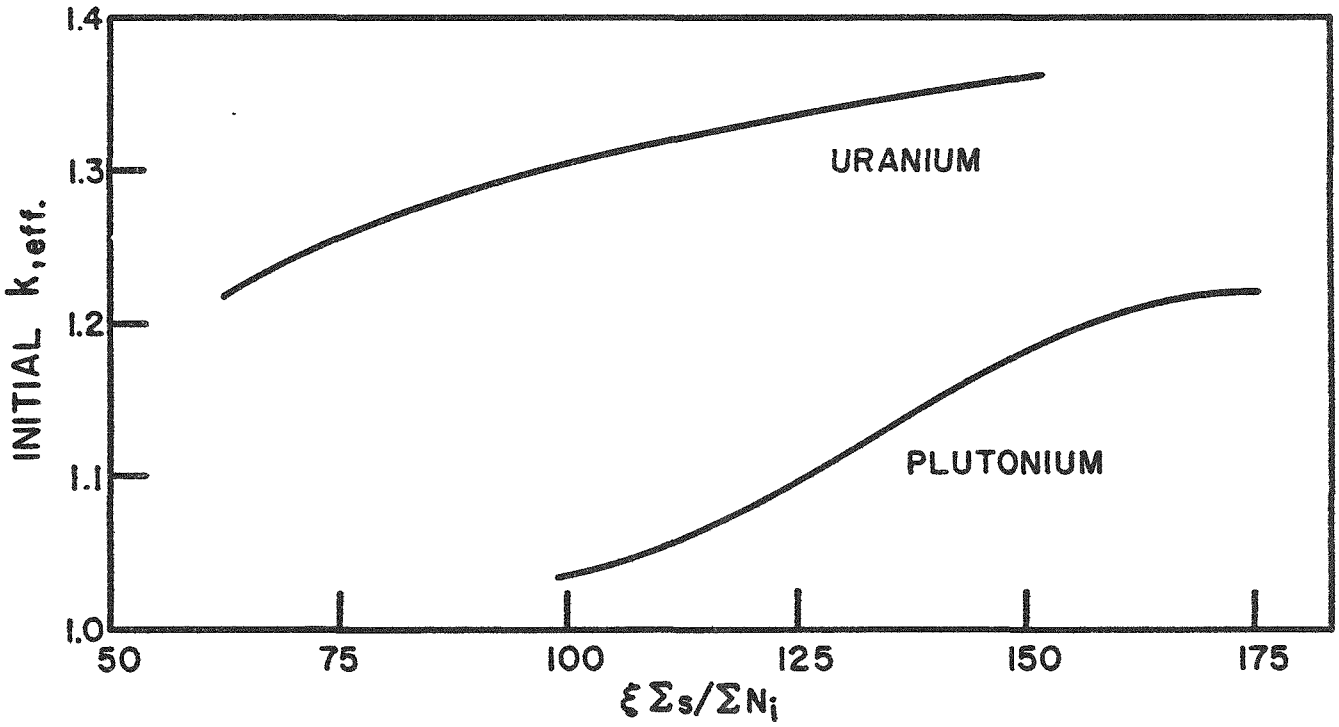

VARIATION OF INITIAL HOT, EQUILIBRIUM FISSION PRODUCT Keff. WITH DEGREE OF MODERATION UNDER CONDITIONS THAT YIELD OPTIMUM FUEL CYCLE COSTS

Figure 8.4

PREPARATION AND COATING OF SPHERICAL OXIDE PARTICLES

Task 11.00
C. S. Caldwell L. J. Jones

Preparation of Spherical PuO_2 Particles from Ceramic Grade Powders
(A. Biancheria)

During the current reporting period, agglomeration methods for forming spherical particles from ceramic grade PuO_2 as a starting material have been further investigated. Densification after forming was obtained by high-temperature sintering or by partial sintering followed by plasma torch melting. Spherical high density materials will be used initially for coating studies and later for dispersion fuel fabrication development. The current goal is to prepare 100 gm quantities of high and intermediate density particles within the 80-170 mesh range utilizing dry-agglomeration followed by sintering at temperatures up to 1650°C. Previous work using a dry-pressing breakdown forming method gave spherical particles of intermediate density after sintering at 1500°C in air(i).

Several trials have been made employing PuO_2 Sample Pu-297-9 Lot 4 for which powder properties are summarized in Table 11.1. Three separate portions of the powder were subjected to a variety of attrition procedures including wet and dry vibratory mix milling or ball milling. The dry powder was then agglomerated and shaped by rolling in a jar for 10-30 minutes. Two of the portions yielded very low quantities of +120 mesh spheres although yields of up to 35% were obtained in the -120 +200 mesh range. The third portion, designated as B-3, gave a 35% yield of +120 mesh green spheres on the first agglomeration cycle. Over half of this material was in the -70 +100 mesh range, and acceptable sphericity was obtained as shown in Figure 11.1. By forcing the oversize material through a 120 mesh screen and recycling this material in combination with the -120 mesh fines, larger spherical agglomerates were prepared. Utilizing four complete cycles in this manner, -50 +70 mesh green spheres were prepared with an overall yield of 28%.

Although green agglomerate shapes were uniformly spherical, a significant percentage of the resulting sintered spheres (Figures 11.2 and 11.3) exhibited distortions thought to be caused by local green density variations. In addition, doublet formation due to particle-particle sintering was observed; this effect can be minimized by using alternate pre-sintering

---

(i) NUMEC P-70, Progress Report, "Development of Plutonium-Bearing Fuel Materials", p. 73.

Table 11.1

Characteristics of PuO_2 Powder
Used for Mechanical Sphere Forming

Sample Designation	Bulk Density gm/cc	Tap Density gm/cc	Average Particle Size*, microns	Surface Area M^2/gm
297-Pu-9 Lot 4A	2.22	2.87	3.3	6.6

* Recalcined

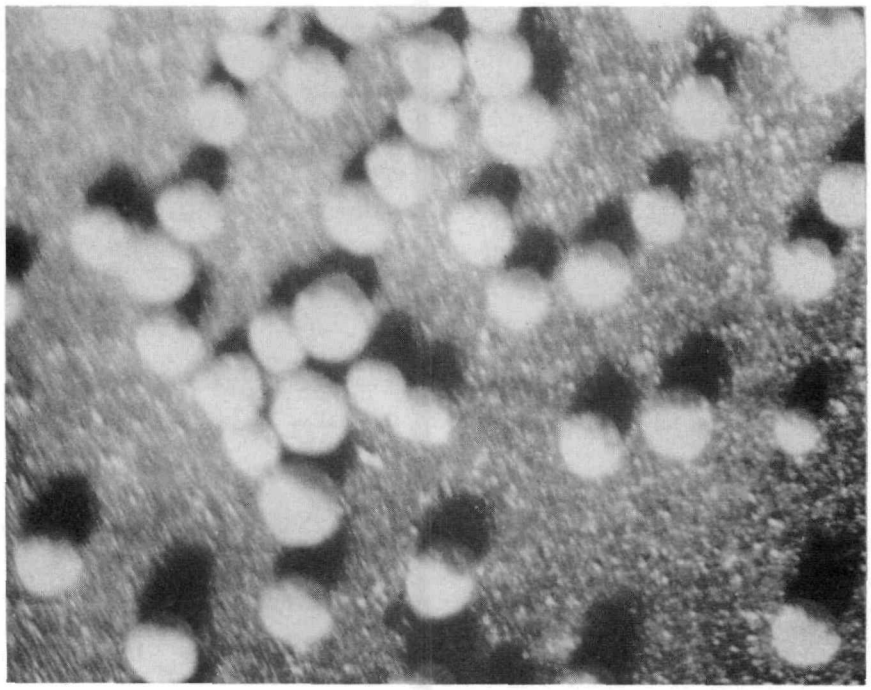

Figure 11.1

Agglomerate-formed PuO_2 Spheres Prior to Sintering
(-70+120 mesh)

Sample B-3-15 40X

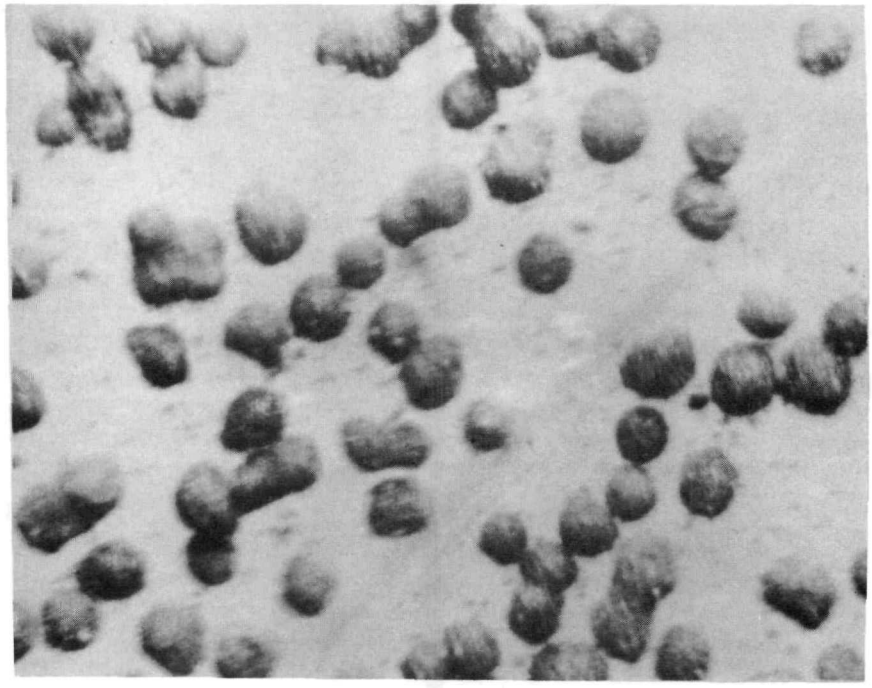

Figure 11.2

Agglomerate-formed PuO_2 Spheres after Sintering
(-70+120 mesh fraction)

Sample B-3-15S 40X

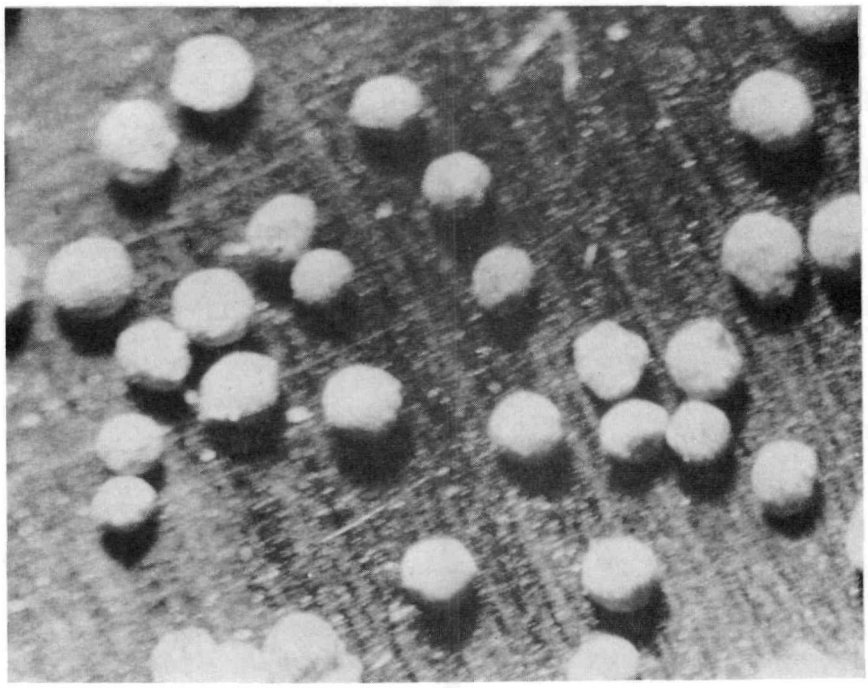

Figure 11.3

Agglomerate-formed PuO_2 Spheres
after Sintering

Sample B-3-12S 40X

conditions. The densities and sintering conditions of several representative samples are summarized in Table 11.2. Information on a representative oversize (-40 +50 mesh) fraction is also included for comparison. The higher density obtained for Sample B-3-15 over that obtained for B-3-12 may be due to the effect of sintering in an oxidizing environment; therefore, direct comparisons on several samples will be made to clarify this effect.

Production of Spherical PuO_2 by Plasma Torch
(R. M. Horgos)

Since the last progress report was issued, considerable progress has been made in the development of techniques to produce spherical particles by the plasma torch. During early trials on PuO_2[(i)], there had been an indication that a severe decrease in particle size could be expected due to either poor thermal shock resistance of the PuO_2 or to an undesirable characteristic of the standard feed mechanism which tended to pulverize the feed particles prior to their introduction to the plasma flame. Upon modification of the feed mechanism and subsequent spheroidization trials, it was concluded that the poor previous results had been due primarily to the method of feeding.

Although modification of the feed system increased the yield of on-sized particles, the operating efficiency as to number of spheres formed was unaffected when utilizing torch operating conditions similar to those used for the original trials. Under these conditions, yields of on-size spherical particles were only about 25 to 30%. To increase the yields, a systematic study was initiated to determine the optimum feed materials and operating torch parameters. While early observations indicated the best feed material to be pre-rolled spheres[(ii)], continued investigation has shown that any type of feed material can be converted to a satisfactory product by proper choice of torch current and gas flows.

From an economical viewpoint, the most desirable type of feed material would be previously unprocessed powders having a particle size near to the desired size of the final product. The homogeneous precipitation studies reported under Task 2.00 are directed towards this application. Unsintered ceramic-grade powder would be too friable, and particle forming with subsequent sintering to at least 35 to 50% of theoretical density would be required. Crushing of high-fired, high-density pellets must be ruled out on economic grounds, since it has been shown that a loss of 40 to 50% results due to fines.

(i) NUMEC P-90, Progress Report, "Development of Plutonium-Bearing Fuel Materials", pp. 68 and 69.

(ii) NUMEC P-90, Progress Report, "Development of Plutonium-Bearing Fuel Materials", p. 73.

Table 11.2

Green and Sintered Densities of Spheroidized PuO_2

Sample Number	Size Range (mesh)	Density gm/cc*		Sintering Conditions		
		Green	Sintered	Atmosphere	Max. Temp, °C	Time at Max. Temp (hr)
B-3-12	-50 +70	3.59	6.8	N_2-6% H_2	1500	2
B-3-15	-70 +120	3.63	9.5	Air	1500	2
B-3-B	-40 +50	-	8.3	N_2-6% H_2	1600	2

* Pycnometric method employing mercury

Subsequent spheroidization trials using sintered PuO_2 agglomerates as feed have resulted in attainment of a high density product. The particular agglomerates utilized were formed by slug pressing unsintered PuO_2 to low pressures, manual granulation through sieves about three sieve sizes larger than the desired end product, and furnace sintering for one hour at 1500 to 1600°C. The measured density of this material was 85 to 90% of theoretical; the density after plasma torch fusion and spheroidization increased to about 92-95%. Representative cross-sections of material produced during these trials are shown in Figures 11.4-11.6. As shown in Figure 11.6, an appreciable increase in density has been realized over earlier trials; 90 to 95% of these particles are completely fused, and essentially 100% are spherical. Continued refinements in torch operating parameters and subsequent processing of the product should allow further improvement in density.

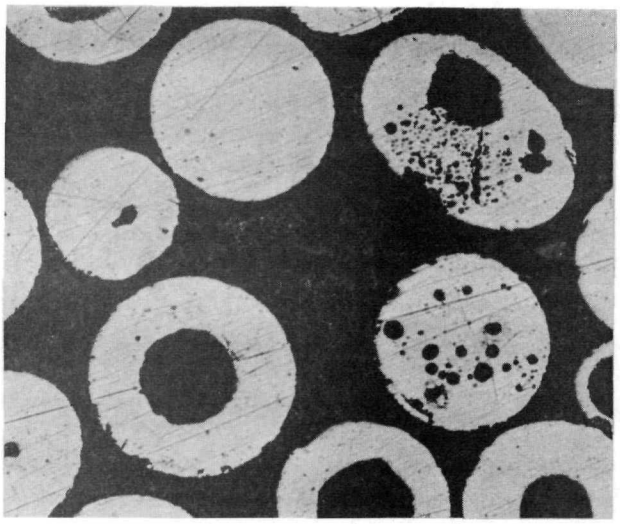

Figure 11.4

PuO_2 Spheroidized in the Plasma Torch
Sintered Agglomerate Feed

Neg. 37 200X

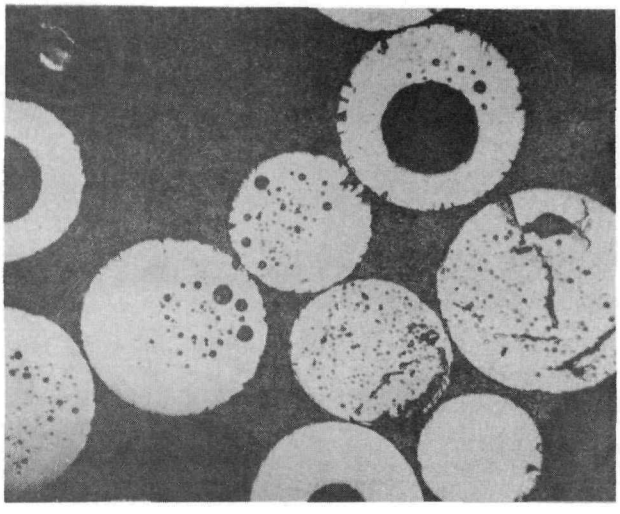

Figure 11.5

PuO_2 Spheroidized in the Plasma Torch
Sintered Agglomerate Feed

Neg. 38 200X

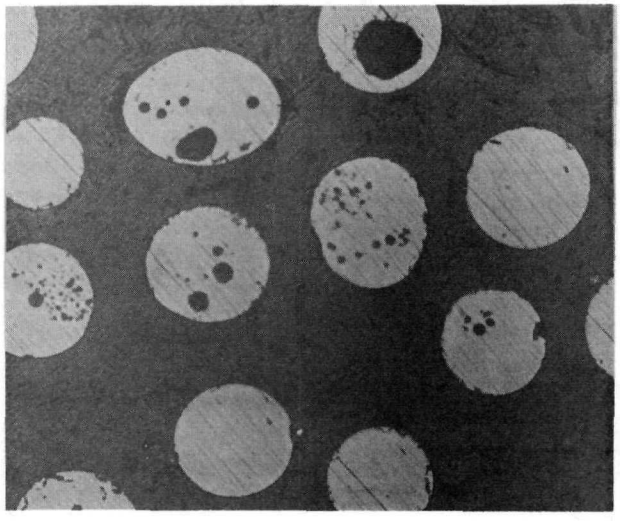

Figure 11.6

PuO_2 Spheroidized in the Plasma Torch
Sintered Agglomerate Feed
and Improved Torch Parameters

Neg. 40 200X